Retained pine density shapes short-term carbon reallocation after thinning and broadleaved enrichment in a Pinus massoniana plantation

Zeyao Zhao

zhao11767966470163.com

Huazhong Agriculture University https://orcid.org/0000-0002-5230-735X

Ning An
Wenjun Xie
Nan Jiang
Zhaogui Yan
Li Mei

Research Article

Keywords: Pinus massoniana, Thinning and mixed planting, Ecosystem carbon reallocation, Retained pine density, Broadleaved enrichment, Soil microbial activity

Posted Date: July 15th, 2026

DOI: https://doi.org/10.21203/rs.3.rs-10248240/v1

Retained pine density shapes short-term carbon reallocation after thinning and broadleaved enrichment in a *Pinus massoniana* plantation

Zeyao Zhao[a], Ning An[b], Wenjun Xie[a], Nan Jiang[a], Zhaogui Yan[a], Li Mei[a] *

[a] College of Horticulture and Forestry Sciences/Hubei Engineering Technology Research Center for Forestry Information, Huazhong Agricultural University, Wuhan 430070, China

[b] Experimental Center of Tropical Forestry, Chinese Academy of Forestry, Pingxiang 532600, China

* Email of the corresponding author: meili@mail.hzau.edu.cn

Abstract

Background and aims

Thinning and mixed planting treatment (TMPT) is used to transform pure *Pinus massoniana* plantations, but its short-term effects on plant carbon allocation and topsoil nutrient microbial conditions remain unclear. We tested whether retained pine density controlled ecosystem carbon gain or carbon reallocation after broadleaved enrichment.

Methods

We compared an unthinned Control (750 pine stems ha^{-1}) with four TMPT levels (MP600, MP450, MP300, MP150) that retained 600, 450, 300, or 150 pine stems ha^{-1}, respectively, and receiving 300 native broadleaved seedlings ha^{-1}. Six years later, we measured stand structure, ecosystem carbon stocks, soil properties, microbial biomass, and enzyme activities.

Results

TMPT increased tree size variation, size inequality, and species mingling more strongly than stem spatial structure. Retained pines were larger at lower densities, but pine carbon per unit area declined. MP300 and MP150 reduced ecosystem carbon by 22% and 41%, respectively. MP600 retained pine carbon near the Control but did not maintain ecosystem carbon. MP450 maintained ecosystem carbon near the Control (88 vs. 92 Mg ha^{-1}) despite 22% lower pine carbon, because soil carbon was 19% higher and understory and mean broadleaved carbon were highest. Retained pine density explained pine carbon (R^2 = 0.885) and ecosystem carbon (R^2 = 0.845), but

not soil or broadleaved carbon. MP450 had 38% higher soil organic carbon, 52% higher microbial biomass carbon, and 56–65% higher C, N, and P acquiring enzyme activities than the Control.

Conclusion

TMPT caused short-term carbon reallocation rather than uniform carbon gain. Density substitution under MP450 best balanced mature pine carbon retention with higher topsoil and non-pine vegetation carbon.

Keywords: *Pinus massoniana*; Thinning and mixed planting; Ecosystem carbon reallocation; Retained pine density; Broadleaved enrichment; Soil microbial activity.

1 Introduction

Forest ecosystems store approximately 80% of aboveground and 70% of belowground terrestrial organic carbon, making them a cornerstone of global climate-change mitigation (Dixon et al., 1994; Pan et al., 2011; Pan et al., 2024). In managed plantations, however, the key issue is not only how much carbon is stored, but where that carbon is retained. Carbon is distributed among tree biomass, understory vegetation, litter, and soil. These pools respond differently to stand development and silvicultural intervention. Recent syntheses further show that the global forest carbon sink depends strongly on forest demography, disturbance history, and management, rather than on biomass accumulation alone (Keenan et al., 2016; Pugh et al., 2019; Heinrich et al., 2023). Thus, plantation carbon responses should be evaluated not only as changes in total ecosystem carbon, but also as carbon reallocation among tree, understory, litter, and soil pools.

Transforming monoculture plantations can redistribute carbon by changing stand structure and species composition. Pure stands accumulate tree biomass rapidly, but maintain simple community composition, size structure, and spatial organization. Such structural simplicity limits carbon transfer beyond the dominant tree layer and suppresses understory development, litter diversity, nutrient cycling, and soil carbon retention (Brancalion and Holl, 2020). Mixed-species forests often show higher productivity, stronger resource complementarity, and more active nutrient cycling than monocultures, but these effects depend on species identity, stand density, site conditions, and stand age (Paquette and Messier, 2010; Forrester, 2014; Liang et al.,

2016; Ammer, 2018; Augusto and Boča, 2022). Plantation transformation should therefore be viewed not simply as adding species, but as changing how carbon is distributed among the dominant tree layer, introduced trees, understory vegetation, litter, and soil.

Thinning creates the central carbon trade-off in plantation transformation: it releases growing space but immediately removes mature tree carbon. By reducing retained pine density, thinning can lower competition for light, water, and nutrients and thereby promote the size growth of remaining trees. It can also increase canopy openness, alter soil microclimate, and create space for understory vegetation and introduced broadleaved trees (Lei et al., 2021; Cheng et al., 2025). These structural changes matter for carbon storage because forest carbon is often linked to stand structural complexity and soil conditions. In mixed oak–pine forests, structural diversity explained ecosystem carbon storage more strongly than species diversity alone (Fatunsin and Naka, 2025). Likewise, in tropical and subtropical forests, stand structure and soil properties jointly shape aboveground and belowground carbon stocks (Ali et al., 2019; Aponte et al., 2020; Sandra et al., 2025). However, thinning also removes carbon already stored in mature pine stems, branches, foliage, and roots. This immediate removal can reduce area based tree carbon in the short-term, even when the retained trees become larger after competition release. The carbon consequence of thinning therefore depends on whether gains in retained trees, understory vegetation, litter, soil, and introduced broadleaved trees can compensate for carbon removed from the dominant pine layer (Zhang et al., 2018; Zhang et al.,

2024; Qu et al., 2025).

Broadleaved enrichment can add new carbon pathways, but its contribution depends on the density and competitive environment created by thinning. Introducing broadleaved species changes species composition and can add carbon through broadleaved biomass, understory development, litter inputs, fine roots, and rhizosphere processes. These changes may alter litter quality, rooting patterns, nutrient cycling, and soil carbon formation (Forrester, 2014; Augusto and Boča, 2022).

Previous mixed-plantation studies show why this response is likely to be context dependent. Mixed stands often store more aboveground biomass than monocultures, but belowground responses are less consistent because soil carbon reflects the balance between organic inputs, microbial processing, and decomposition. Species identity is especially important in subtropical plantations, where introduced broadleaved species may differ strongly from *P. massoniana* in litter quality, rooting strategy, and nutrient demand. In highly weathered subtropical soils, phosphorus limitation can further make belowground responses depend more on species traits than on richness alone (Li et al., 2026). For example, a mixed *Castanopsis hystrix–P. massoniana* plantation in Guangxi stored more ecosystem carbon than a pure *P. massoniana* plantation under comparable conditions (He et al., 2013). However, broadleaved enrichment can contribute substantially to ecosystem carbon only if the introduced trees establish and acquire enough resources under the residual pine canopy. Thus, the carbon effect of mixed planting should depend not only on which species are introduced, but also on how many mature pines remain after thinning.

How thinning and broadleaved enrichment interact through retained pine density remains a key uncertainty in plantation carbon management. When a fixed number of broadleaved seedlings is added after thinning, different retained pine densities create different total post treatment densities. High pine retention with broadleaved addition can increase total stand density, moderate pine retention can substitute broadleaved trees for removed pines, and stronger pine removal can reduce total stand density (Osei et al., 2021; Che et al., 2024; Li et al., 2026). These configurations are likely to create different resource environments and different carbon balances. Densification may retain more pine carbon but intensify competition for light, water, and nutrients, whereas density substitution may reduce pine dominance without increasing total stem density. By contrast, stronger density reduction may release more growing space but remove too much mature pine carbon to be compensated in the short-term (Thurm and Pretzsch, 2021; Del Río et al., 2022; Han et al., 2025). However, most plantation studies have evaluated thinning or enrichment planting as broad management categories, rather than testing whether different retained pine densities shift ecosystem carbon through stand densification, density substitution, or net density reduction. This leaves two linked gaps. First, we still know little about how TMPT reallocates carbon among pine, soil, broadleaved, understory, and litter pools. Second, it remains unclear whether soil carbon follows pine density driven carbon loss or instead covaries with soil nutrients, microbial biomass, and enzyme activity (Xu et al., 2024; Lin et al., 2025; Qu et al., 2025; Zhang et al., 2026).

Pinus massoniana plantations provide a suitable system for testing how retained pine

density shapes carbon reallocation during broadleaved enrichment. As the dominant plantation type in southern China, *P. massoniana* plantations are increasingly transformed through thinning and broadleaved enrichment to improve stand quality and ecological function (He et al., 2013; Lei et al., 2021; Li et al., 2026). In our study area, pure *P. massoniana* stands were thinned to four retained pine density levels and then interplanted with 300 stems ha^{-1} of three native broadleaved species: *Mytilaria laosensis*, *Erythrophleum fordii*, and *Castanopsis hystrix*. Six years after treatment, we quantified spatial and non-spatial stand structure, carbon stocks of major ecosystem components, soil physicochemical properties, microbial biomass, and enzyme activities. We tested whether TMPT increased ecosystem carbon stock or instead reallocated carbon among pine, soil, broadleaved, understory, and litter pools. We hypothesized that: (i) TMPT would increase tree size variation, tree-size inequality, and species mingling more strongly than stem spatial arrangement; (ii) stronger thinning would reduce ecosystem carbon because pine carbon loss would exceed gains in soil and non-pine pools, whereas MP450 would maintain a more balanced carbon distribution through density substitution; and (iii) pine and ecosystem carbon would track retained pine density, whereas soil carbon would covary more strongly with soil nutrients, microbial biomass, and enzyme activity.

2 Materials and methods

2.1 Study area

This study was conducted at the Experimental Center of Tropical Forestry in Pingxiang, Guangxi, China (22°03′ N, 106°52′ E). The region has a humid subtropical monsoon climate with clear wet and dry seasons. Mean annual air temperature ranges

from 20.5 to 21.7 °C. Mean annual precipitation ranges from 1200 to 1500 mm, with most rainfall occurring from April to September. Mean annual sunshine duration ranges from 1200 to 1600 h. Mean annual evaporation ranges from 1200 to 1400 mm. Mean annual relative humidity ranges from 80 to 84% (http://www.nmc.cn/). The area is dominated by low mountains and hills. The soils are lateritic red soils (Ferralsols, World Reference Base for Soil Resources) and are usually deeper than 80 cm (Liu et al., 2025). The zonal vegetation is subtropical evergreen broadleaved forest, although the current landscape is mainly composed of plantations.

2.2 Experimental design and treatments

Pure *Pinus massoniana* plantations were established in 2006 at an initial planting density of 750 stems ha^{-1}. In 2018, thinning created a gradient of retained pine densities: 600, 450, 300, and 150 stems ha^{-1}, alongside an unthinned control (750 stems ha^{-1}). The five treatments were designated Control, MP600, MP450, MP300, and MP150.

Immediately after thinning in 2018, the four thinned treatments (MP600–MP150) were interplanted with two-year-old seedlings of three native broadleaved species: *Mytilaria laosensis* (90 stems ha^{-1}), *Erythrophleum fordii* (90 stems ha^{-1}), and *Castanopsis hystrix* (120 stems ha^{-1}), totaling 300 stems ha^{-1}. No interplanting occurred in the Control. Hereafter, these combined treatments are referred to as the thinning and mixed planting treatments (TMPT). Total post treatment density was therefore 900, 750, 600, and 450 stems ha^{-1} in MP600, MP450, MP300, and MP150, respectively. Relative to the initial planting density, total density increased in MP600, remained unchanged in MP450, and decreased in MP300 and MP150.

2.3 Sampling plot establishment and stand inventory

In July 2024, three independent sampling plots were randomly established within each treatment, totaling 15 plots (5 treatments × 3 plots). Each plot measured 20 m × 30 m, and plots were at least 200 m apart. To minimize environmental heterogeneity among plots, all plots were located on south facing slopes with comparable topography and soil conditions.

Within each plot, all live trees with diameter at breast height (DBH) ≥ 3 cm were identified to species, and DBH (1.3 m above ground) was recorded to the nearest 0.1 cm. The x–y coordinates of each tree were recorded for spatial mapping and structural index calculation. Crown width was measured along the east–west and north–south axes, and the mean of these two measurements was used as crown width. For retained *P.massoniana* trees, total tree height and height to crown base (HCB) were also measured to characterize individual tree size.

2.4 Stand structural indices

To quantify non-spatial structural indices (Qin et al., 2022; Miao et al., 2025), we calculated four plot level indices, the coefficient of variation of DBH (CV) (Eq. 1), skewness (SK) (Eq. 2), the Gini coefficient (GC) (Eq. 3), and the Shannon-Wiener size diversity index (H) (Eq. 4). Together, these indices quantify variation, asymmetry, inequality, and size class diversity in tree size distribution.

$$CV = \frac{SD_{DBH}}{Mean_{DBH}} \quad (1)$$

$$GC = \frac{\sum_{i=1}^{n}(2i - n - 1)DBH_i}{n\sum DBH_i} \quad (2)$$

$$SK = \frac{\sum(DBH_i - Mean_{DBH})^3}{(n-1)SD^3} \quad (3)$$

$$H = -\sum p_i \, lnp_i \quad (4)$$

where n is the number of trees in a plot. DBH_i is the DBH of tree *i*. Mean DBH is the plot mean DBH. SD is the sample standard deviation of DBH, and p_i is the proportion of trees in the *i*th DBH class.

For each tree within the plot, we identified its four nearest neighbors using horizontal Euclidean distances and then quantified its spatial structure with four nearest neighbor indices (Dong et al., 2022; Liang et al., 2025), the uniform angle index (W) (Eq. 5), dominance index (U) (Eq. 6), mingling index (M) (Eq. 7), and crowding index (CI) (Eq. 8). Trees in the immediate external buffer zone were surveyed to calculate the indices for trees inside the plot.

$$W = \frac{1}{4n}\sum_{i=1}^{n}\sum_{j=1}^{4} z_{ij}, z_{ij} = \begin{cases} 1, \alpha_j < \alpha_0 = 72^{\circ} \\ 0, otherwise \end{cases} \quad (5)$$

$$U = \frac{1}{4n}\sum_{i=1}^{n}\sum_{j=1}^{4} k_{ij}, k_{ij} = \begin{cases} 1, if\ DBH_j > DBH_i \\ 0, otherwise \end{cases} \quad (6)$$

$$M = \frac{1}{4n}\sum_{i=1}^{n}\sum_{j=1}^{4} v_{ij}, v_{ij} = \begin{cases} 1, sp_j \neq sp_i \\ 0, otherwise \end{cases} \quad (7)$$

$$CI = \frac{1}{4n}\sum_{i=1}^{n}\sum_{j=1}^{4} y_{ij}, y_{ij} = \begin{cases} 1, if\ (CW_i + CW_j) > L_{ij} \\ 0, if\ (CW_i + CW_j) \leq L_{ij} \end{cases} \quad (8)$$

where n is the number of trees in a plot; sp_i and sp_j are the species identities of the reference tree *i* and its *j*th nearest neighbor; DBH_i and DBH_j are their respective diameters; CW_i and CW_j are their crown widths, and L_{ij} is the horizontal distance between their stems. For the indicator variables: $Z_{ij} = 1$ when the angle between adjacent neighbors is smaller than the standard angle $\alpha_0 = 72°$; otherwise, $z_{ij} = 0$. $K_{ij} = 1$ when $DBH_j > DBH_i$; otherwise, $k_{ij} = 0$. $V_{ij} = 1$ when neighbor j belongs to a different species from reference tree *i*; otherwise, $v_{ij} = 0$. $Y_{ij} = 1$ when $CW_i + CW_j > L_{ij}$; otherwise, $y_{ij} = 0$.

2.5 Understory vegetation, litter, and tree organ sampling

To estimate carbon stocks across ecosystem components, we sampled understory vegetation, surface litter, and tree organs for carbon concentration measurements in July 2024. Three 1 m × 1 m subplots were established in each plot. All understory vegetation was harvested and separated into aboveground and belowground components. Surface litter was concurrently collected from these same subplots. These samples were transported to the laboratory, cleaned of adhering soil and debris, and oven dried at 105 °C to constant mass to determine dry biomass.

For the tree layer, stem wood, branches, leaves, and fine roots were sampled from three representative trees per species in each plot. For each species, the selected trees had DBH values close to the corresponding plot mean. In total, 180 organ samples were collected for *Pinus massoniana* across all five treatments (5 treatments × 3 replicate plots × 3 trees × 4 organs). Across the four TMPT, the three interplanted broadleaved species (*Mytilaria laosensis*, *Erythrophleum fordii*, and *Castanopsis hystrix*) were additionally sampled, yielding 432 broadleaved organ samples (4

treatments × 3 replicate plots × 3 species × 3 trees × 4 organs). For each organ, approximately 100 g of fresh material was collected and oven dried at 105 °C to constant mass.

All dried plant and litter samples were finely milled to pass an 80-mesh sieve before chemical analysis. Total carbon (TC) was determined using the potassium dichromate oxidation method.

2.6 Soil sampling and physicochemical analyses

Soil from the 0-20 cm layer was sampled in July 2024 after litter removal using two complementary approaches: undisturbed core sampling for soil physical properties and auger sampling for soil chemical properties, microbial biomass, and enzyme activities.

For the undisturbed core sampling, three replicate cores were collected from each plot using stainless steel rings, totaling 45 ring core samples (5 treatments × 3 plots ×3 replicates ring samples). Soil water content (SWC) was measured gravimetrically after oven drying at 105 °C to constant mass. Soil bulk density (SBD) and soil capillary porosity (SCP) were calculated based on core volumes and weights at saturation, after free drainage, and after oven drying (Qi et al., 2022).

For the auger sampling, three replicate soil samples were collected per plot, yielding 45 augered samples. The augered samples were placed in an ice box and transported to the laboratory, hand sorted to remove roots and debris, homogenized, and passed through a 2-mm sieve. The sieved sample was divided into two subsamples. One subsample was air-dried for pH, soil organic carbon (SOC), total nitrogen (TN), and total phosphorus (TP). The other subsample was stored at 4 °C for microbial biomass and enzyme analyses.

For the air-dried subsamples, soil pH was measured in a 1:2.5 soil-to-water suspension using a calibrated glass electrode meter (Zhang et al., 2020). SOC was determined by the potassium dichromate oxidation method (Bao, 2000), soil TN was determined by the Kjeldahl digestion procedure (Bao, 2000), and soil TP was determined by the molybdenum blue colorimetric method after acid digestion (Bao, 2000).

For the 4 °C subsamples, MBC, MBN, and MBP were measured by the chloroform fumigation extraction method (Joshi and Garkoti, 2023; Zheng et al., 2023). Fresh soil was fumigated with ethanol free $CHCl_3$ for 24 h. Fumigated and non-fumigated soils were extracted with 0.5 mol L^{-1} K_2SO_4 (For MBC and MBN) or with 0.5 mol L^{-1} $NaHCO_3$ at pH 8.5 (For MBP). MBC, MBN, and MBP were calculated as the difference between fumigated and non-fumigated extracts divided by k_{EC} = 0.45, k_{EN} = 0.54, and k_{EP} = 0.40, respectively.

Also using the 4 °C subsamples, β-1,4-glucosidase (BG), β-1,4-N-acetylglucosaminidase (NAG), and acid phosphatase (ACP) activities were assayed with substrate specific microplate methods (Wu et al., 2023). Briefly, a homogeneous soil slurry was prepared by suspending 1.5 g of fresh soil in 100 mL of sodium acetate buffer (50 mmol L^{-1}, pH 4.5), followed by vortexing for 1 min and stirring for 1 h. For each assay, 200 μL of the soil slurry and 50 μL of the corresponding substrate solution were added to a 96-well microplate. The specific substrates used were p-nitrophenyl-β-D-glucopyranoside for BG, 4-methylumbelliferyl-N-acetyl-β-D-glucosaminide for NAG, and disodium phenyl phosphate for ACP. After incubation in the dark at 20 °C for 4 h, the reactions were terminated with 10 μL 1 mol L^{-1} NaOH. Enzyme activities were measured using a multifunctional microplate reader and expressed on an oven dry soil basis.

For all soil variables, the three replicate values within each plot were averaged to obtain one plot level value before statistical analysis.

2.7 Estimation of biomass and carbon stocks

Tree biomass was estimated for each inventoried tree using species-specific allometric equations (Table S1; Luo et al. 2020). Plot level organ biomass was then obtained by summing the estimated biomass of all trees within each plot and converting it to a hectare basis. Carbon stocks for the tree, understory, and litter components were then calculated by multiplying their respective dry biomass by these measured TC concentrations.

Table S1 Allometric equations used to estimate biomass of *Pinus massoniana* and mixed broadleaved species

289

Tree species	Tree components	Equation form	Coeff. *a*	Coeff. *b*	*R*
Pinus massoniana					
	Stem wood	$W = a \times D^b$	0.054	2.466	0.979
	Stem bark	$W = a \times D^b$	0.039	1.761	0.853
	Total branch	$W = a \times D^b$	0.005	2.704	0.916
	Total leaf	$W = a \times D^b$	0.009	2.002	0.658
	Total root	$W = a \times D^b$	0.023	2.232	0.943
Mixed species					
	Total stem	$W = a \times b^D$	0.2228	1.6465	0.964
	Total branch	$W = a + b \times D^4$	0.3601	0.00022233	0.91
	Total leaf	$W = a + b \times D^4$	0.2568	0.00011544	0.915
	Total root	$W = a + b \times D^2$	0.4154	0.0792	0.918

290

291 W: biomass (kg); D: diameter at breast height (DBH, cm). a and b are fitted equation
292 coefficients, and R indicates the goodness of fit of each allometric model.

293

294 Carbon stocks for the retained *P. massoniana* (C_{pine}) and the mixed broadleaved
295 species ($C_{broadleaf}$) were calculated using Eqs. 9 and 10 (Moraes et al., 2026).

$$C_{pine}(kg\ ha^{-1}) = \sum_{org=1}^{4} \left(B_{pine,org}(kg\ ha^{-1}) \times TC_{pine,org}(g\ kg^{-1}) \right) / 1000 \quad (9)$$

$$C_{broadleaf}(kg\ ha^{-1}) = \sum_{spe=1}^{3} \sum_{org=1}^{4} \left(B_{broadleaf(spe),org}(kg\ ha^{-1}) \times TC_{broadleaf(spe),org}(g\ kg^{-1}) \right) / 1000 \quad (10)$$

296 where *org* represents the specific tree organ (1 = stem, 2 = branch, 3 = leaf, and 4 =
297 root), and *spe* represents the three interplanted broadleaved species (*Mytilaria*
298 *laosensis*, *Erythrophleum fordii*, and *Castanopsis hystrix*). B (kg ha^{-1}) and TC (g kg^{-1})
299 denote the dry biomass and total carbon concentration of the corresponding organ and
300 species, respectively. The constant 1000 is a unit conversion factor. Stem biomass

was calculated as the sum of stem wood and stem bark biomass, and the measured stem carbon concentration was applied to the combined stem biomass.

The carbon stocks of the understory vegetation and litter layers were calculated using Eqs. 11 and 12, respectively (Moraes et al., 2026).

$$C_{understory} = \sum_{comp=1}^{2} (B_{understory,comp}\,(kg\ ha^{-1}) \times TC_{understory,comp}(g\ kg^{-1}))/1000 \quad (11)$$

$$C_{litter} = B_{litter}(kg\ ha^{-1}) \times TC_{litter}(g\ kg^{-1}))/1000 \quad (12)$$

where *comp* represents the aboveground and belowground components of the herbaceous understory. The constant 1000 is a unit conversion factor.

The soil carbon stock (C_{soil}, kg ha^{-1}) was calculated using Eq. 13 (Joshi and Garkoti, 2023; Moraes et al., 2026).

$$C_{soil}(kg\ ha^{-1}) = SOC(g\ kg^{-1}) \times SBD(g\ cm^{-3}) \times Depth(cm) \times 100 \quad (13)$$

where SOC is the soil organic carbon concentration (g kg^{-1}). SBD is soil bulk density (g cm^{-3}), and Depth is soil thickness (20 cm). The constant 100 is a unit conversion factor.

Ecosystem carbon stock (C_{eco}) was defined as the the measured tree, understory, litter, and soil carbon pools using Eq. 14 (Moraes et al., 2026).

$$C_{eco} = C_{tree} + C_{understory} + C_{litter} + C_{soil} \quad (14)$$

To facilitate comparison and visualization, the carbon stock values were subsequently converted from kg ha^{-1} to Mg ha^{-1} by dividing by 1000.

2.8 Statistical analyses

All statistical analyses were conducted in R version 4.4.1 (R Core Team 2024). Data were tested for normality and homogeneity of variance using the Shapiro–Wilk test and Levene's test, respectively. Variables that violated these assumptions were log10

transformed before analysis (He et al., 2024). Unless otherwise stated, data are presented as means ± SE, and significance was accepted at $P < 0.05$.

One-way ANOVA was used to test treatment effects on stand structural indices, pine size variables, individual pine biomass, ecosystem component biomass, carbon concentrations, carbon stocks, soil physicochemical properties, microbial biomass, and enzyme activities. When the ANOVA indicated significant treatment effects, means were separated using Duncan's multiple range test in the *agricolae* package (De Mendiburu and Simon, 2015).

To facilitate comparisons among response variables measured in different units, we quantified treatment effects relative to the Control using Hedges' g. Effect sizes were calculated for both carbon stock variables and soil physicochemical properties. For each response variable, Hedges' g was calculated from plot level values by comparing each TMPT directly with the Control (n = 3 plots per treatment). The pooled (combined) standard deviation was calculated using Eq. 15 (Gardner et al., 2019; Leverkus et al., 2021).

$$S_p = \sqrt{\frac{(n_t - 1)S_t^2 + ((n_c - 1)S_c^2}{n_t + n_c - 2}} \quad (15)$$

S_t and S_c are the standard deviations of the TMPT and Control groups, respectively. n_t and n_c are their sample sizes.

The uncorrected standardized mean difference was calculated using Eq. 16 (Hedges, 1981; Gardner et al., 2019).

$$d = (\bar{X}_t - \bar{X}_c)/S_p \quad (16)$$

where $\bar{X}_t$ and $\bar{X}_c$ are the treatment and Control means, respectively,

and Hedges' g was obtained using Eq. 17 (Willms et al., 2017; Gardner et al., 2019).

$$g = J \times d,\ J = 1 - \frac{3}{4(n_t+n_c)-9} \quad (17)$$

where J is the small sample correction factor. Positive and negative values of Hedges' g indicate increases and decreases relative to the Control, respectively. Hedges' g was used to show effect direction and magnitude. For the Hedges' g analysis of $C_{broadleaf}$, Control values were set to zero because broadleaved trees were absent from the Control plots. Statistical significance was evaluated from the original plot level data using one-way ANOVA and Duncan's multiple range test.

Regression analyses were used to evaluate the relationships between retained pine density and carbon stocks (C_{eco}, C_{soil}, C_{pine}, $C_{broadleaf}$, $C_{understory}$, and C_{litter}). For each carbon pool, we first fitted a linear model and then tested whether the addition of a quadratic term improved model fit. The quadratic model was retained only when the quadratic term was significant; otherwise, the linear model was used. The fitted equation, coefficient of determination (R^2), and P value were reported. For $C_{broadleaf}$, Control plots were shown for reference but were excluded from model fitting because broadleaved species were absent in the Control.

Principal component analysis (PCA) was used to summarize coordinated variation in pH, TN, TP, MBC, MBN, MBP, BG, NAG, and ACP. All variables were standardized to zero mean and unit variance before PCA because they were measured in different units. SOC and SBD were excluded because both variables were used to calculate C_{soil}, whereas SWC and SCP were analyzed separately as soil physical properties. The first principal component (PC1) was used to represent the soil nutrient microbial axis. A linear regression was used to examine the relationship between the soil nutrient microbial axis and C_{soil} using plot level observations across all treatments. A quadratic term was also tested but was retained only if it significantly improved model fit. The fitted equation, R^2, P value, and 95% confidence interval were reported. Separate linear regressions between C_{soil} and MBC, MBN, MBP, BG, NAG, and ACP were retained as supplementary analyses.

3 Results

3.1 TMPT increased tree size variation, size inequality, and species mingling

The thinning and mixed planting treatments (TMPT: MP600, MP450, MP300, and

MP150) increased tree-size inequality and species mingling more consistently than they changed stem spatial arrangement (Fig. 1). MP600, MP450, MP300, and MP150 had higher CV values relative to the Control (0.53, 0.54, 0.66, and 0.81 vs. 0.13; $P < 0.05$) and higher GC values relative to the Control (0.28, 0.29, 0.35, and 0.40 vs. 0.07; $P < 0.05$). MP300 had a lower SK than the Control (0.08 vs. 0.32; $P < 0.05$), whereas MP150 had a higher SK (0.79 vs. 0.32; $P < 0.05$). The treatments did not differ in H. Among the spatial indices, the TMPT affected M and CI but not W or U (Fig. 1b). MP600, MP450, MP300, and MP150 increased M from 0.00 in the Control to 0.56, 0.59, 0.69, and 0.70, respectively. MP300 and MP150 produced the highest M values and both exceeded MP600 (0.69 and 0.70 vs. 0.56; $P < 0.05$). MP150 reduced CI by 34–37% relative to the Control, MP600, and MP450 (0.58 vs. 0.88, 0.89, and 0.92; $P < 0.05$). In contrast, W and U did not differ among treatments.

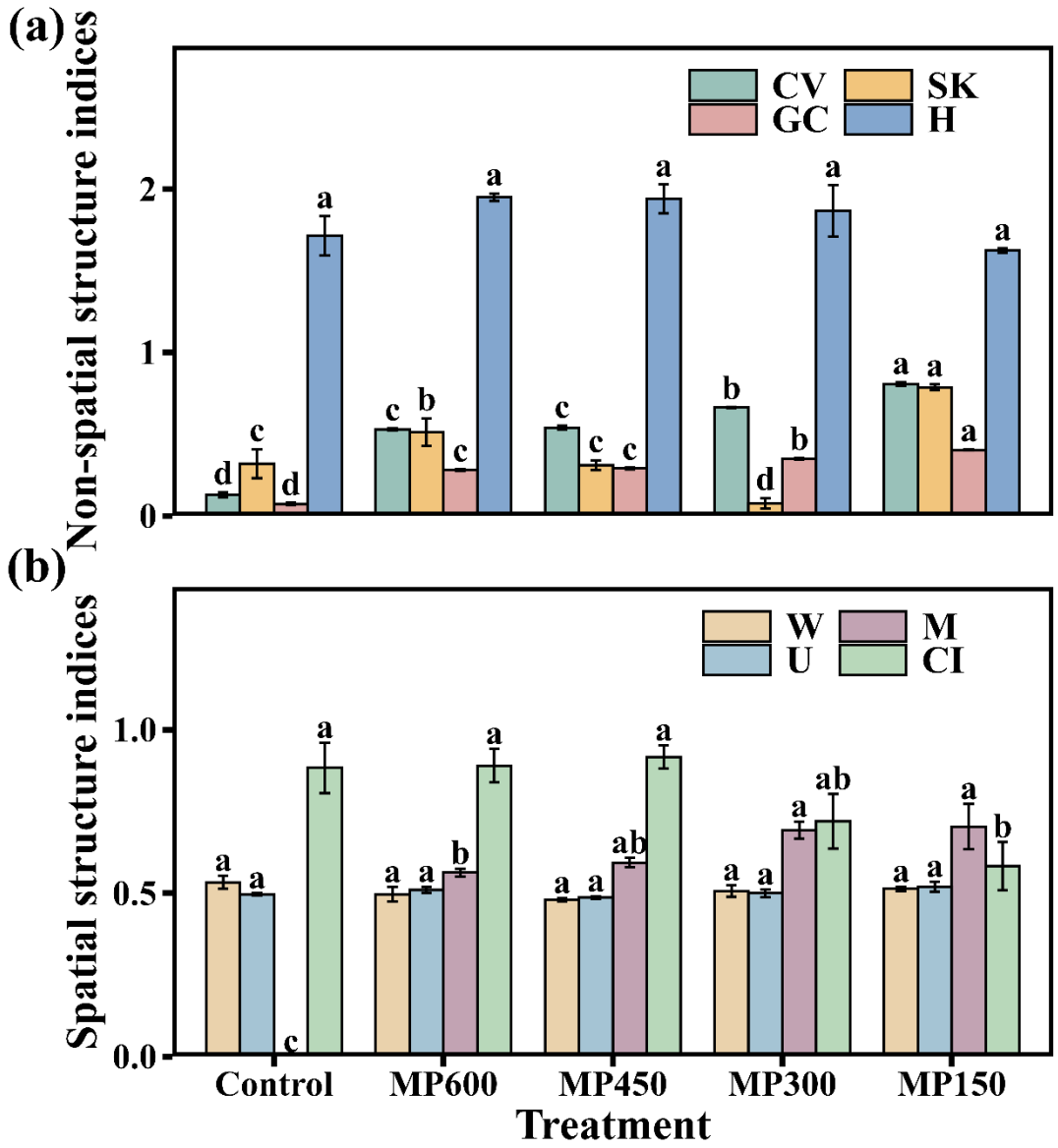

Fig. 1 Stand structural indices under the five experimental treatments in the *Pinus massoniana* plantation. (a) Non-spatial structural indices; (b) Spatial structural indices. Values are means ± SE (n = 3). Different lowercase letters indicate significant differences among treatments at $P < 0.05$. CV: Coefficient of variation of DBH; SK: Skewness; GC: Gini coefficient; H: Shannon–Wiener size diversity index; W: Uniform angle index; U: Dominance index; M: Mingling index; CI: Crowding index. Control: Unthinned pure *P. massoniana* plantation; MP600–MP150: thinning and mixed planting treatments retaining 600 to 150 *P. massoniana* stems ha^{-1}.

3.2 Retained pines were larger at lower densities, but area based pine carbon declined

Retained pines were larger at lower retained densities (Table S2). Mean DBH increased from 22.5 cm in the Control to 24.1, 25.0, 26.2, and 26.9 cm in MP600, MP450, MP300, and MP150, respectively ($P < 0.05$). Mean tree height increased from 20.20 m in the Control to 21.7–24.2 m across the TMPT, and mean crown width increased from 5.7 to 6.1–6.9 m ($P < 0.05$). HCB was higher in MP450, MP300, and MP150 than in the Control, whereas MP600 did not differ from the Control. Mean individual pine biomass increased progressively as retained density declined, from 182 kg tree^{-1} in the Control to 214, 232, 263, and 280 kg tree^{-1} in MP600, MP450, MP300, and MP150, respectively.

The increase in individual pine biomass did not maintain pine carbon per unit area (Table 1; Tables S2–S5). C_{pine} was 53.69 Mg ha^{-1} in MP600 and did not differ from the Control (56.86 Mg ha^{-1}), but declined to 44.64, 34.78, and 18.21 Mg ha^{-1} in MP450, MP300, and MP150, respectively ($P < 0.05$). This contrast was clearest for stem biomass: individual stem biomass increased from 129.66 kg tree^{-1} in the Control to 199.25 kg tree^{-1} in MP150, whereas area based stem carbon declined from 40.64 to 12.96 Mg ha^{-1}. Area based branch, leaf, and root carbon showed the same decline with decreasing retained pine density.

Table 1 Ecosystem and component carbon stocks under the five treatments

Components	Treatments

	Control	MP600	MP450	MP300	MP150
C_{eco} (Mg ha^{-1})	92.03 ± 3.66a	82.39 ± 3.54b	88.48 ± 1.87ab	71.57 ± 1.53c	54.61 ± 2.25d
C_{soil} (Mg ha^{-1})	33.52 ± 1.15b	26.11 ± 0.69c	39.94 ± 0.65a	33.36 ± 0.81b	33.39 ± 1.54b
C_{pine} (Mg ha^{-1})	56.86 ± 4.15a	53.69 ± 2.89a	44.64 ± 0.96b	34.78 ± 2.25c	18.21 ± 0.69d
$C_{broadleaf}$ (Mg ha^{-1})	-	0.75 ± 0.03b	1.33 ± 0.20a	1.05 ± 0.15ab	0.98 ± 0.01ab
$C_{understory}$ (Mg ha^{-1})	1.00 ± 0.01c	1.11 ± 0.03c	1.56 ± 0.06a	1.29 ± 0.04b	1.13 ± 0.09bc
C_{litter} (Mg ha^{-1})	0.66 ± 0.01c	0.73 ± 0.04c	1.00 ± 0.06ab	1.09 ± 0.02a	0.92 ± 0.01b

Values are means ± SE (n = 3). Different lowercase letters within a row indicate significant differences among treatments at $P < 0.05$. C_{eco}: Ecosystem carbon stock; C_{soil}: Soil carbon stock; C_{pine}: *Pinus massoniana* carbon stock; $C_{broadleaf}$: Mixed broadleaved species carbon stock; $C_{understory}$: Understory vegetation carbon stock; C_{litter}: Litter carbon stock. Control: Unthinned pure *P. massoniana* plantation; MP600–MP150: thinning and mixed planting treatments retaining 600 to 150 *P. massoniana* stems ha^{-1}.

Table S2 Growth traits and individual biomass of retained *P. massoniana* trees under the five treatments

Properties	Treatments				
	Control	MP600	MP450	MP300	MP150
DBH (cm)	22.48 ± 0.47d	24.06 ± 0.62c	24.98 ± 0.24bc	26.22 ± 0.39ab	26.93 ± 0.59a
Tree height (m)	20.2 ± 0.43d	21.65 ± 0.56c	22.47 ± 0.21bc	23.6 ± 0.36ab	24.24 ± 0.53a
Crown width (m)	5.71 ± 0.13d	6.13 ± 0.16c	6.36 ± 0.05bc	6.69 ± 0.1ab	6.86 ± 0.16a
HCB (m)	10.47 ± 0.25d	11.14 ± 0.38cd	11.57 ± 0.05bc	12.12 ± 0.19ab	12.56 ± 0.24a

Branch (kg plant^{-1})	23.55 ± 1.47d	28.13 ± 1.8cd	30.71 ± 0.55bc	35.36 ± 1.74ab	38.01 ± 2.24a
Stem (kg plant^{-1})	129.66 ± 7.12d	152.13 ± 8.83cd	164.83 ± 2.81bc	186.73 ± 8ab	199.25 ± 10.5a
Leaf (kg plant^{-1})	4.66 ± 0.2d	5.32 ± 0.26cd	5.71 ± 0.09bc	6.31 ± 0.21ab	6.66 ± 0.29a
Root (kg plant^{-1})	24.52 ± 1.23d	28.44 ± 1.54cd	30.66 ± 0.5bc	34.37 ± 1.33ab	36.5 ± 1.77a
Total (kg plant^{-1})	182.38 ± 10.04d	214.02 ± 12.43cd	231.91 ± 3.95bc	262.77 ± 11.29ab	280.43 ± 14.8a

Values are means ± SE (n = 3). Different lowercase letters within a row indicate significant differences among treatments at $P < 0.05$. DBH, diameter at breast height; HCB, height to crown base. Biomass values represent individual pine biomass. Refer to Table 1 for treatment details.

Table S3 Carbon stocks of plant components under five treatments

Carbon stocks	Treatments				
	Control	**MP600**	**MP450**	**MP300**	**MP150**
Pinus massoniana					
Branch (kg ha^{-1})	7664.51 ± 639.78a	7325.20 ± 458.74ab	6145.84 ± 145.54b	4872.82 ± 348.32c	2567.39 ± 112.52d
Stem (kg ha^{-1})	40639.59 ± 2953.05a	38240.77 ± 2060.39a	31745.68 ± 719.28b	24736.44 ± 1596.54c	12963.98 ± 466.69d
Leaf (kg ha^{-1})	1484.24 ± 98.45a	1379.99 ± 66.01a	1131.37 ± 11.48b	861.18 ± 46.36c	445.28 ± 17.51d
Root (kg ha^{-1})	7067.22 ± 456.38a	6741.36 ± 315.10a	5618.53 ± 93.75b	4307.61 ± 264.51c	2229.53 ± 88.94d
Mytilaria laosensis					
Branch (kg ha^{-1})	-	24.12 ± 1.34a	43.25 ± 9.42a	34.30 ± 9.90a	30.30 ± 0.70a
Stem (kg ha^{-1})	-	160.33 ± 15.52a	406.27 ± 129.30a	297.99 ± 134.26a	231.72 ± 11.07a
Leaf (kg ha^{-1})	-	14.15 ± 0.64a	23.55 ± 4.46a	19.15 ± 4.63a	17.08 ± 0.31a
Root (kg ha^{-1})	-	101.59 ± 5.86b	156.74 ± 25.49a	128.44 ± 23.10ab	123.05 ± 2.08ab
Erythrophleum fordii					
Branch (kg ha^{-1})	-	20.83 ± 0.30b	25.66 ± 0.53a	24.40 ± 0.96a	25.01 ± 0.62a
Stem (kg ha^{-1})	-	114.28 ± 3.14b	163.07 ± 5.93a	150.85 ± 9.47a	159.67 ± 5.55a
Leaf (kg ha^{-1})	-	11.95 ± 0.08b	14.31 ± 0.24a	13.63 ± 0.39a	13.81 ± 0.25a
Root (kg ha^{-1})	-	94.26 ± 1.94b	118.19 ± 2.62a	112.07 ± 4.38a	114.99 ± 1.87a
Castanopsis hystrix					

Branch (kg ha^{-1})	-	23.17 ± 0.39c	33.13 ± 1.28a	26.66 ± 0.54b	26.10 ± 0.17b
Stem (kg ha^{-1})	-	86.03 ± 3.49c	188.24 ± 13.10a	122.95 ± 8.40b	119.06 ± 2.62b
Leaf (kg ha^{-1})	-	13.48 ± 0.14c	18.07 ± 0.65a	15.08 ± 0.34b	14.68 ± 0.10b
Root (kg ha^{-1})	-	81.51 ± 2.11c	137.50 ± 5.67a	104.36 ± 3.49b	101.49 ± 1.80b
Understory					
Aboveground (kg ha^{-1})	442.47 ± 13.29c	510.41 ± 22.40bc	743.04 ± 37.22a	610.31 ± 10.53b	544.62 ± 63.14bc
Belowground (kg ha^{-1})	557.27 ± 13.84c	600.23 ± 4.51c	821.28 ± 23.68a	682.11 ± 38.17b	583.72 ± 28.55c

Values are means ± SE (n = 3). Different lowercase letters within a row indicate significant differences among treatments at $P < 0.05$. Refer to Table 1 for treatment details.

Table S4 Carbon concentrations of plant and litter components under five treatments

Carbon concentration	Treatments				
	Control	**MP600**	**MP450**	**MP300**	**MP150**
Pinus massoniana					
Branch (g kg^{-1})	442.00 ± 2.17bc	438.00 ± 2.17bc	450.00 ± 2.17a	444.00 ± 2.17ab	437.00 ± 2.17c
Stem (g kg^{-1})	426.00 ± 2.17b	423.00 ± 2.17b	433.00 ± 2.17a	427.00 ± 2.17ab	421.00 ± 2.17b
Leaf (g kg^{-1})	433.00 ± 2.00c	436.00 ± 2.00bc	446.00 ± 2.00a	440.00 ± 2.00b	432.00 ± 2.00c
Root (g kg^{-1})	392.00 ± 2.00d	399.00 ± 2.00bc	412.00 ± 2.00a	404.00 ± 2.00b	395.00 ± 2.00cd
Mytilaria laosensis					
Branch (g kg^{-1})	-	415.00 ± 2.17b	421.00 ± 2.17ab	425.00 ± 2.17a	422.00 ± 2.17a
Stem (g kg^{-1})	-	405.00 ± 2.17b	412.00 ± 2.17a	416.00 ± 2.17a	411.00 ± 2.17ab
Leaf (g kg^{-1})	-	388.00 ± 2.00c	396.00 ± 2.00ab	399.00 ± 2.00a	392.00 ± 2.00bc
Root (g kg^{-1})	-	357.00 ± 2.00b	362.00 ± 2.00ab	366.00 ± 2.00a	361.00 ± 2.00ab
Erythrophleum fordii					
Branch (g kg^{-1})	-	427.00 ± 2.17bc	438.00 ± 2.17a	432.00 ± 2.17ab	425.00 ± 2.17c
Stem (g kg^{-1})	-	396.00 ± 2.17b	405.00 ± 2.17a	399.00 ± 2.17ab	394.00 ± 2.17b
Leaf (g kg^{-1})	-	378.00 ± 2.00bc	390.00 ± 2.00a	383.00 ± 2.00b	375.00 ± 2.00c
Root (g kg^{-1})	-	392.00 ± 2.00bc	402.00 ± 2.00a	396.00 ± 2.00b	389.00 ± 2.00c
Castanopsis hystrix					

Branch (g kg^{-1})	-	447.00 ± 2.17b	456.00 ± 2.17a	451.00 ± 2.17ab	445.00 ± 2.17b
Stem (g kg^{-1})	-	390.00 ± 2.17b	398.00 ± 2.17a	393.00 ± 2.17ab	388.00 ± 2.17b
Leaf (g kg^{-1})	-	382.00 ± 2.00bc	392.00 ± 2.00a	386.00 ± 2.00b	378.00 ± 2.00c
Root (g kg^{-1})	-	372.00 ± 2.00b	382.00 ± 2.00a	376.00 ± 2.00b	370.00 ± 2.00b
Understory					
Aboveground (g kg^{-1})	395.00 ± 2.00d	405.00 ± 2.00c	432.00 ± 2.00a	418.00 ± 2.00b	408.00 ± 2.00c
Belowground (g kg^{-1})	350.00 ± 2.00bc	345.00 ± 2.00cd	370.00 ± 2.00a	355.00 ± 2.00b	342.00 ± 2.00d
Litter (g kg^{-1})	438.00 ± 2.17c	442.00 ± 2.17abc	448.00 ± 2.17a	445.00 ± 2.17ab	440.00 ± 2.17bc

Values are means ± SE (n = 3). Different lowercase letters within a row indicate significant differences among treatments at $P < 0.05$. Refer to Table 1 for treatment details.

Table S5 Biomass of plant and litter components under five treatments

Properties	Treatments				
	Control	**MP600**	**MP450**	**MP300**	**MP150**
Pinus massoniana					
Branch (kg ha^{-1})	17336.2 ± 1419.16a	16717.16 ± 979.07a	13654.34 ± 229.23b	10975.98 ± 794.18b	5877 ± 278.07c
Stem (kg ha^{-1})	95420.25 ± 7090.67a	90402.84 ± 4806.74a	73301.04 ± 1163.45b	57946.63 ± 3864.87c	30808.4 ± 1285.73d
Leaf (kg ha^{-1})	3426.82 ± 219.09a	3164.5 ± 143.53a	2537.05 ± 36.62b	1958.44 ± 115.34c	1030.37 ± 35.14d
Root (kg ha^{-1})	18040.96 ± 1256.05a	16900.61 ± 840.7a	13637.32 ± 208.2b	10664.86 ± 672.78c	5643.64 ± 215.43d
Total biomass (kg ha^{-1})	134224.23 ± 9983.95a	127185.11 ± 6767.19a	103129.75 ± 1637.31b	81545.91 ± 5446.05c	43359.41 ± 1813.26d
Mytilaria laosensis					
Branch (kg ha^{-1})	0.00 ± 0.00b	58.12 ± 3.21a	102.70 ± 22.38a	80.40 ± 22.62a	71.83 ± 2.05a
Stem (kg ha^{-1})	0.00 ± 0.00b	395.77 ± 37.43a	984.63 ± 310.94a	716.83 ± 323.37a	563.81 ± 27.02a
Leaf (kg ha^{-1})	0.00 ± 0.00b	36.46 ± 1.67a	59.61 ± 11.62a	48.03 ± 11.74a	43.58 ± 1.06a
Root (kg ha^{-1})	0.00 ± 0.00b	284.68 ± 17.36a	432.58 ± 68.70a	351.50 ± 64.98a	340.93 ± 7.22a
Total biomass (kg ha^{-1})	0.00 ± 0.00b	775.03 ± 59.62a	1579.51 ± 413.32a	1196.76 ± 422.73a	1020.15 ± 36.92a
Erythrophleum fordii					
Branch (kg ha^{-1})	0.00 ± 0.00c	48.80 ± 0.84b	58.60 ± 1.24a	56.48 ± 1.97a	58.82 ± 1.16a
Stem (kg ha^{-1})	0.00 ± 0.00d	288.72 ± 9.92b	402.63 ± 14.30a	377.98 ± 22.88a	405.20 ± 13.35a
Leaf (kg ha^{-1})	0.00 ± 0.00c	31.62 ± 0.44b	36.71 ± 0.64a	35.61 ± 1.02a	36.82 ± 0.60a
Root (kg ha^{-1})	0.00 ± 0.00d	240.48 ± 5.16b	294.00 ± 6.00a	282.96 ± 10.35a	295.64 ± 5.70a
Total biomass (kg ha^{-1})	0.00 ± 0.00c	609.62 ± 16.38b	791.93 ± 22.20a	753.02 ± 36.23a	796.49 ± 20.81a
Castanopsis hystrix					

Branch (kg ha^{-1})	0.00 ± 0.00d	51.82 ± 0.64c	72.64 ± 2.68a	59.12 ± 1.49b	58.66 ± 0.56b
Stem (kg ha^{-1})	0.00 ± 0.00d	220.58 ± 8.78c	472.75 ± 31.28a	312.54 ± 18.49b	306.85 ± 6.69b
Leaf (kg ha^{-1})	0.00 ± 0.00d	35.28 ± 0.33c	46.09 ± 1.39a	39.07 ± 0.77b	38.83 ± 0.29b
Root (kg ha^{-1})	0.00 ± 0.00d	219.17 ± 6.44c	359.91 ± 14.36a	277.73 ± 11.48b	274.26 ± 3.84b
Total biomass (kg ha^{-1})	0.00 ± 0.00d	526.85 ± 16.18c	951.40 ± 49.73a	688.46 ± 32.24b	678.61 ± 11.35b
Understory					
Aboveground (kg ha^{-1})	1120.03 ± 30.68c	1260.01 ± 51.88bc	1720.02 ± 86.39a	1459.95 ± 20.3ab	1335.54 ± 158.42bc
Belowground (kg ha^{-1})	1591.91 ± 32.03c	1739.98 ± 20.58bc	2220.03 ± 69.73a	1920.04 ± 93.42b	1707.69 ± 91.93bc
Total biomass (kg ha^{-1})	2711.95 ± 23.37c	2999.99 ± 71.23bc	3940.05 ± 155.97a	3380 ± 102.47b	3043.24 ± 250.34bc
Litter biomass (kg ha^{-1})	1500.03 ± 18.12c	1650.01 ± 83.75c	2228.18 ± 133.82b	2460.03 ± 32.07a	2080.04 ± 20.77b

Values are means ± SE (n = 3). Different lowercase letters within a row indicate significant differences among treatments at $P < 0.05$. Refer to Table 1 for treatment details.

3.3 MP450 maintained ecosystem carbon despite lower pine carbon

Ecosystem carbon was lower under MP600, MP300, and MP150, whereas MP450 maintained a value comparable to the Control (Figs. 2 and 3; Table 1). Relative to the Control, C_{eco} was 10%, 22%, and 41% lower in MP600, MP300, and MP150, respectively (82.39, 71.57, and 54.61 vs. 92.03 Mg ha^{-1}; $P < 0.05$). In contrast, Ceco did not differ between MP450 and the Control (88.48 vs. 92.03 Mg ha^{-1}). The decline in C_{eco} under stronger thinning was accompanied by lower C_{pine}. Relative to the

Control, MP450, MP300, and MP150 had 22%, 39%, and 68% lower C_{pine}, respectively (44.64, 34.78, and 18.21 vs. 56.86 Mg ha^{-1}; $P < 0.05$), whereas MP600 maintained C_{pine} at a level comparable to the Control.

MP450 combined lower pine carbon with higher soil and non-pine vegetation carbon. MP450 had 19% higher C_{soil} than the Control (39.94 vs. 33.52 Mg ha^{-1}; $P < 0.05$) and the highest $C_{understory}$ (1.56 Mg ha^{-1}). It also had the highest mean $C_{broadleaf}$ (1.33 Mg ha^{-1}), whereas MP300 had the highest C_{litter} (1.09 Mg ha^{-1}). The Hedges' g analysis showed the same treatment directions as the raw carbon stock values, including negative effects on C_{eco} and C_{pine} and a positive effect on C_{soil} under MP450.

Carbon allocation also differed between MP450 and the Control (Fig. 2). Under MP450, C_{pine} accounted for 50% of C_{eco} and C_{soil} accounted for 45%, compared with 62% and 37%, respectively, in the Control. Accordingly, the combined contribution of soil, broadleaved trees, understory vegetation, and litter increased from 38% in the Control to 50% in MP450.

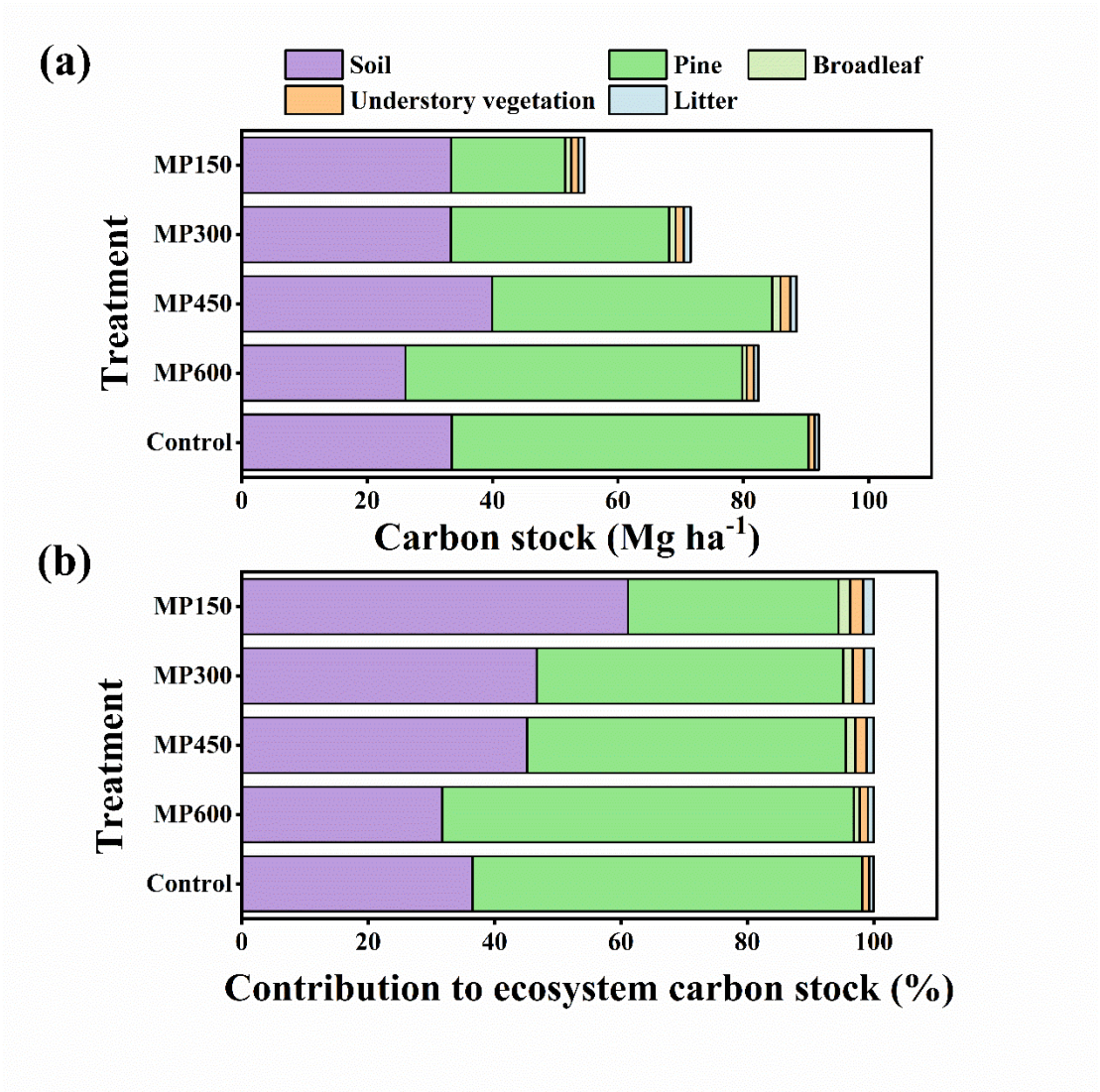

479

480 **Fig. 2** Carbon allocation among ecosystem pools under the five treatments. (a)
481 Absolute carbon stocks of ecosystem components; (b) Relative contribution of each
482 component to ecosystem carbon stock. Stacked bars show the contributions of soil,
483 pine, mixed broadleaved species, understory vegetation, and litter carbon pools. Refer
484 to Fig. 1 for treatment details.

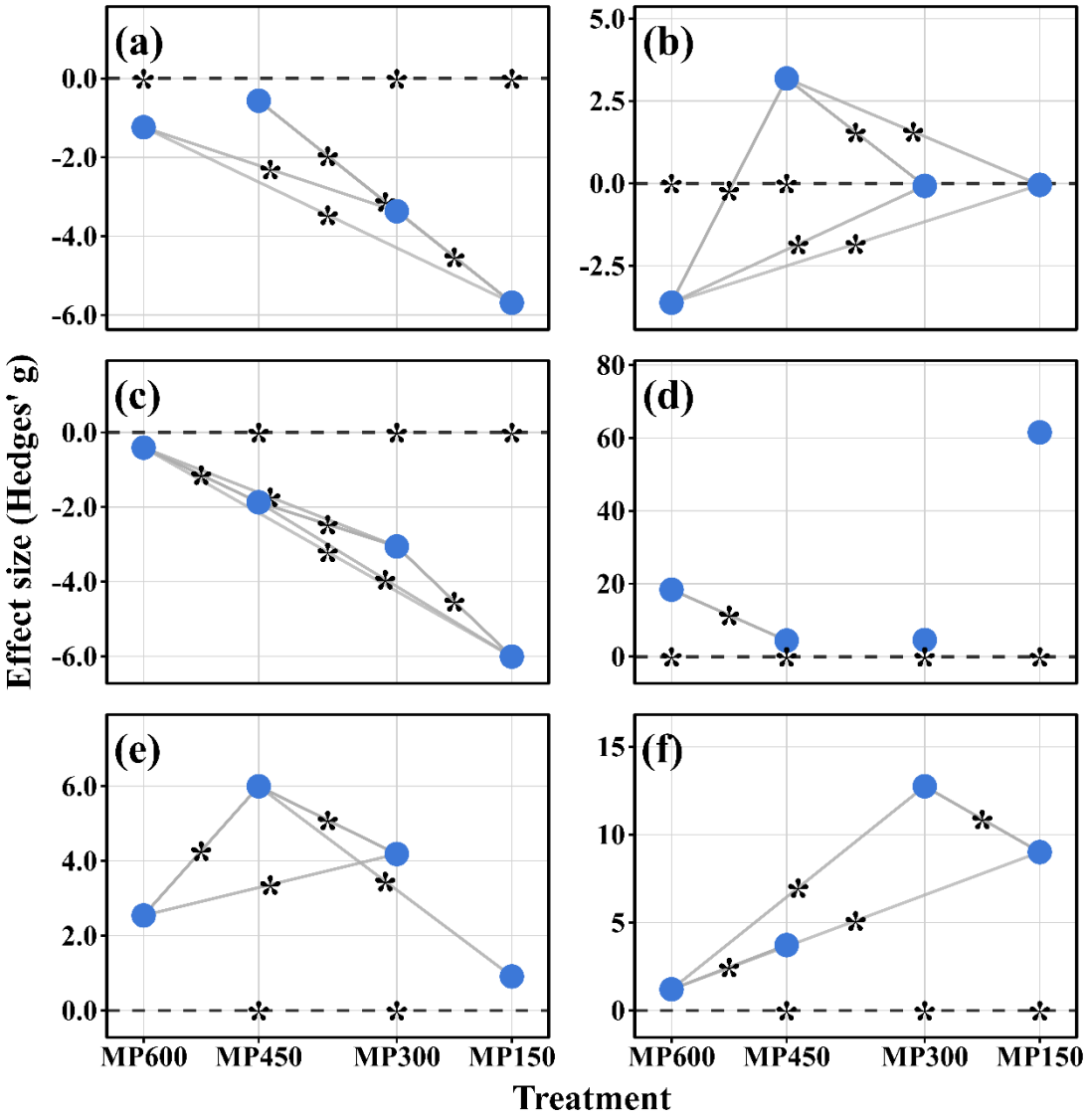

Fig. 3 Standardized effect sizes (Hedges' g) of the four thinning and mixed planting treatments on ecosystem and component carbon stocks relative to the Control. (a) Ecosystem carbon stock (C_{eco}); (b) Soil carbon stock (C_{soil}); (c) *Pinus massoniana* carbon stock (C_{pine}); (d) Mixed broadleaved species carbon stock ($C_{broadleaf}$); (e) Understory vegetation carbon stock ($C_{understory}$); (f) Litter carbon stock (C_{litter}). Points represent Hedges' g for each treatment relative to the Control. The horizontal dashed line at zero indicates no treatment effect. Positive and negative values indicate increases and decreases relative to the Control, respectively. Asterisks indicate significant differences in the original plot level data among treatments, as determined by one-way ANOVA followed by Duncan's multiple range test ($P < 0.05$). Solid lines connect treatment levels that differed significantly in the original data. Refer to Fig. 1

for treatment details.

3.4 Retained pine density was related to pine and ecosystem carbon, but not soil or broadleaved carbon

Carbon pools differed in their relationships with retained pine density (Fig. 4, Fig. S1). C_{eco} showed a significant positive quadratic relationship with retained pine density, but the increase weakened at higher densities ($R^2 = 0.845$, $P < 0.001$). C_{pine} increased linearly with retained pine density ($R^2 = 0.885$, $P < 0.001$). $C_{understory}$ and C_{litter} showed significant unimodal relationships with retained pine density. Their fitted maxima occurred near 450 and 300 stems ha^{-1}, respectively ($R^2 = 0.609$, $P = 0.004$ for $C_{understory}$; $R^2 = 0.762$, $P < 0.001$ for C_{litter}). In contrast, neither C_{soil} nor $C_{broadleaf}$ was significantly related to retained pine density.

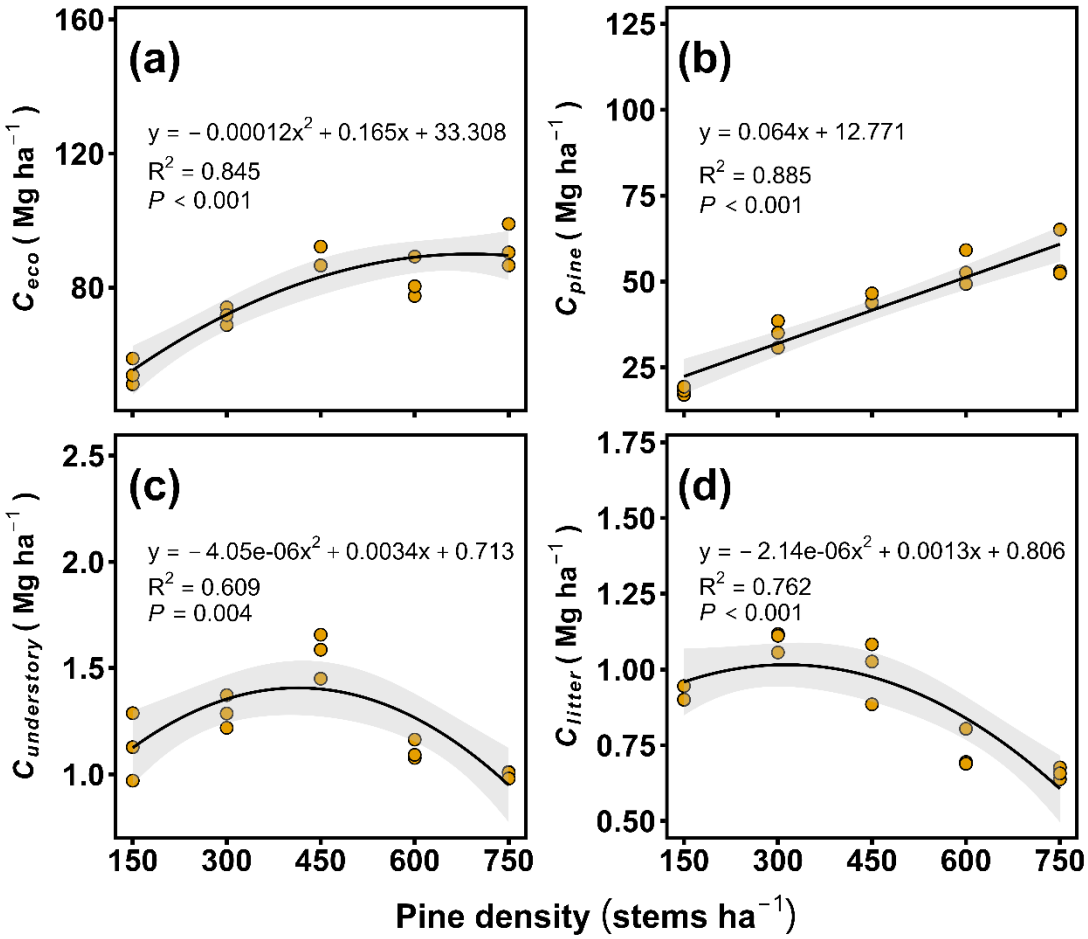

509

510 **Fig. 4** Relationships between retained *P. massoniana* density and selected ecosystem
511 and component carbon stocks across the five treatments. (a) Ecosystem carbon stock
512 (C_{eco}); (b) *Pinus massoniana* carbon stock (C_{pine}); (c) Understory vegetation carbon
513 stock ($C_{understory}$); (d) Litter carbon stock (C_{litter}). Solid lines represent the fitted
514 regression models, and gray shaded areas indicate the 95% confidence intervals.
515 Linear models were fitted first, and quadratic models were retained only when the
516 quadratic term significantly improved model fit. Retained pine density refers to the
517 number of live *P. massoniana* stems retained after thinning. Refer to Fig. 1 for
518 treatment details.

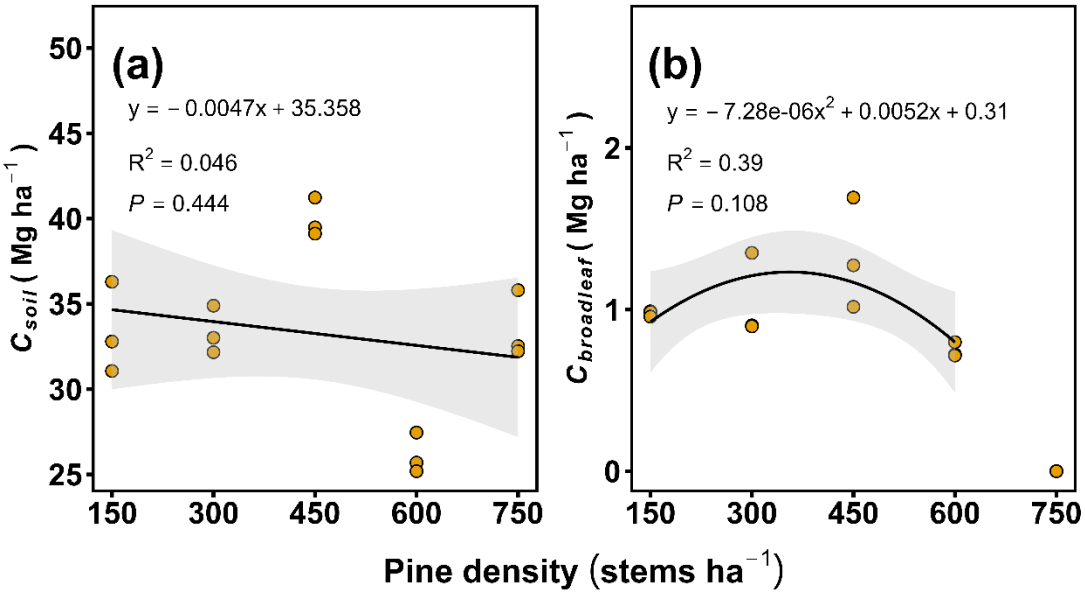

Fig. S1 Relationships between retained *P. massoniana* density and soil and broadleaved carbon stocks. (a) Soil carbon stock (C_{soil}); (b) Mixed broadleaved species carbon stock ($C_{broadleaf}$). Solid lines represent the fitted regression models, and gray shaded areas indicate the 95% confidence intervals. Linear models were fitted first, and quadratic models were retained only when the quadratic term significantly improved model fit. Control observations are shown for reference but were excluded from the $C_{broadleaf}$ model fitting because broadleaved species were absent from the Control. Refer to Fig. 1 for treatment details.

3.5 MP450 had the highest soil carbon, microbial biomass, and enzyme activities

MP450 had the highest SOC and TN concentrations, a higher pH, and a lower SBD than the Control (Fig. 5, Table 2). MP450 had 38% higher SOC and 25% higher TN relative to the Control (18 vs. 13 g kg^{-1}, 1.62 vs. 1.30 g kg^{-1}, respectively; $P < 0.05$). MP450 also had a higher pH than the Control, MP600, and MP150 (4.40 vs. 4.25–4.30; $P < 0.05$), a lower SBD than the Control and MP600 (1.12 vs. 1.29 and 1.24 g cm^{-3}; $P < 0.05$), and a higher TP concentration than the Control and MP600 ($P < 0.05$). Although MP450 had the highest mean SWC and SCP, neither differed significantly from the Control. The Hedges' g analysis showed the same response

directions, with positive effects on pH, SWC, SCP, SOC, TN, and TP and a negative effect on SBD under MP450.

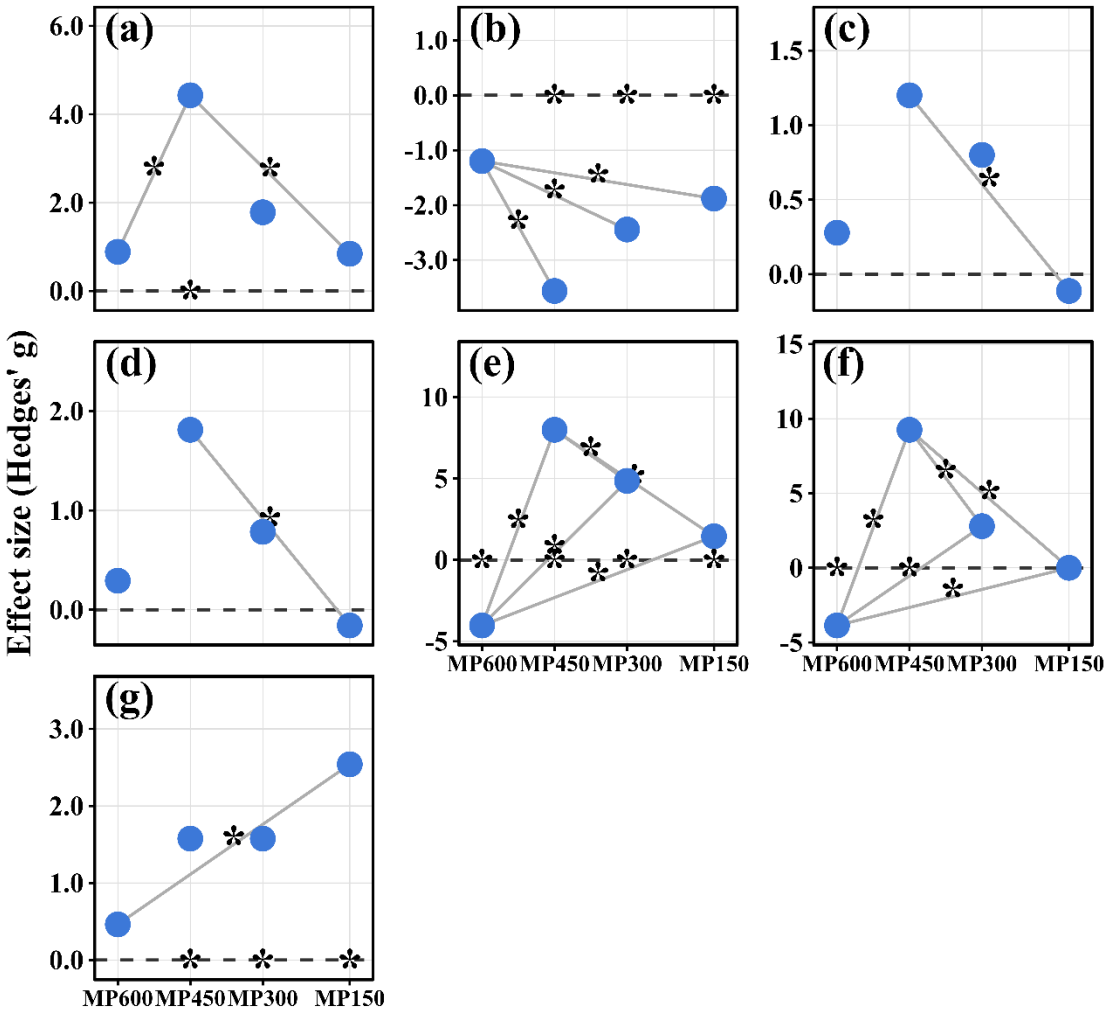

Fig. 5 Standardized effect sizes (Hedges' g) of the four thinning and mixed planting treatments on soil physicochemical properties relative to the Control. (a) pH; (b) Soil bulk density (SBD); (c) Soil water content (SWC); (d) Soil capillary porosity (SCP); (e) Soil organic carbon (SOC); (f) Total nitrogen (TN); (g) Total phosphorus (TP). Points represent Hedges' g for each treatment relative to the Control. The horizontal dashed line at zero indicates no treatment effect. Positive and negative values indicate increases and decreases relative to the Control, respectively. Asterisks indicate significant differences in the original plot level data among treatments, as determined by one-way ANOVA followed by Duncan's multiple range test ($P < 0.05$). Solid lines connect treatment levels that differed significantly in the original data. Refer to Fig. 1

for treatment details.

Table 2 Soil physicochemical properties, microbial biomass, and enzyme activities under the five treatments

Properties	Treatments				
	Control	**MP600**	**MP450**	**MP300**	**MP150**
pH	4.25 ± 0.01b	4.28 ± 0.02b	4.40 ± 0.02a	4.34 ± 0.03ab	4.30 ± 0.04b
SBD (g cm^{-3})	1.29 ± 0.03a	1.24 ± 0.01a	1.12 ± 0.01b	1.14 ± 0.03b	1.13 ± 0.05b
SWC (g g^{-1})	0.29 ± 0.02ab	0.30 ± 0.00ab	0.32 ± 0.01a	0.31 ± 0.01ab	0.29 ± 0.01b
SCP	0.45 ± 0.01ab	0.45 ± 0.01ab	0.48 ± 0.00a	0.47 ± 0.02ab	0.44 ± 0.01b
SOC (g kg^{-1})	12.95 ± 0.16c	10.56 ± 0.35d	17.84 ± 0.37a	14.68 ± 0.17b	14.86 ± 0.84b
TN (g kg^{-1})	1.30 ± 0.01b	1.19 ± 0.02c	1.62 ± 0.02a	1.36 ± 0.01b	1.30 ± 0.04b
TP (g kg^{-1})	0.25 ± 0.01b	0.25 ± 0.01b	0.27 ± 0.01a	0.27 ± 0.01a	0.28 ± 0.01a
MBC (mg kg^{-1})	117.74 ± 1.27c	105.06 ± 2.76d	178.85 ± 2.84a	145.17 ± 1.28b	136.92 ± 6.53b
MBN (mg kg^{-1})	9.56 ± 0.07c	8.69 ± 0.13c	15.24 ± 0.19a	12.10 ± 0.31b	11.46 ± 0.52b
MBP (mg kg^{-1})	7.66 ± 0.08c	6.44 ± 0.07d	11.01 ± 0.10a	9.04 ± 0.03b	8.51 ± 0.49b
BG (nmol g^{-1} h^{-1})	89.26 ± 0.82e	101.82 ± 1.77d	139.69 ± 1.83a	118.90 ± 0.82b	109.31 ± 4.20c
NAG (nmol g^{-1} h^{-1})	35.63 ± 0.41e	40.41 ± 0.89d	58.84 ± 0.91a	48.45 ± 0.41b	44.65 ± 2.10c
ACP (nmol g^{-1} h^{-1})	164.52 ± 1.63e	188.64 ± 3.55d	256.37 ± 3.65a	218.79 ± 1.65b	203.61 ± 8.39c

Values are means ± SE (n = 3). Different lowercase letters within a row indicate significant differences among treatments at $P < 0.05$. SBD: Soil bulk density; SWC: Soil water content; SCP: Soil capillary porosity; SOC: Soil organic carbon; TN: Total nitrogen; TP: Total phosphorus; MBC: Microbial biomass carbon; MBN: Microbial

biomass nitrogen; MBP: Microbial biomass phosphorus; BG: β-1,4-glucosidase; NAG: β-1,4-N-acetylglucosaminidase; ACP: Acid phosphatase. Refer to Table 1 for treatment details.

MP450 also had the highest microbial biomass and enzyme activities among the five treatments (Table 2). MP450 had 52% higher MBC, 59% higher MBN, and 44% higher MBP relative to the Control (179 vs. 118 mg kg^{-1}, 15 vs. 9.56 mg kg^{-1}, and 11 vs. 7.66 mg kg^{-1}, respectively; $P < 0.05$). MP450 also had 56% higher BG activity, 65% higher NAG activity, and 56% higher ACP activity relative to the Control (140 vs. 89 nmol g^{-1} h^{-1}, 59 vs. 36 nmol g^{-1} h^{-1}, and 256 vs. 165 nmol g^{-1} h^{-1}, respectively; $P < 0.05$). MP300 and MP150 maintained intermediate microbial and enzyme values, whereas MP600 had the lowest MBC, MBN, MBP, BG, NAG, and ACP values among the TMPT.

Across treatments, higher C_{soil} was associated with a common gradient of higher soil nutrient concentrations, microbial biomass, and enzyme activities (Fig. 6). PCA summarized the covariation among pH, TN, TP, MBC, MBN, MBP, BG, NAG, and ACP, with PC1 explaining 82.0% of the total variation and PC2 explaining 9.2% (Fig. 6a). C_{soil} increased with PC1 scores, and the linear model explained 62.4% of the variation in C_{soil} ($R^2 = 0.624$, $P < 0.001$, Fig. 6b). C_{soil} also increased significantly with MBC, MBN, MBP, BG, NAG, and ACP in the separate regressions (Fig. S2).

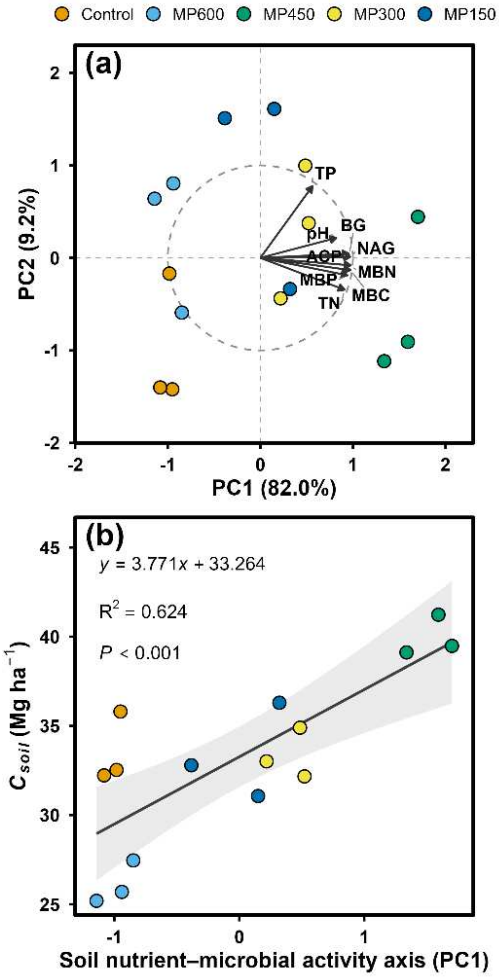

581

582 **Fig. 6** Principal component analysis of soil nutrient and microbial variables and their

583 relationship with soil carbon stock across the five treatments. (a) Principal component

584 analysis of soil nutrient properties, microbial biomass, and enzyme activities; (b)

585 Relationship between the first principal component and soil carbon stock. Points

586 represent individual plots, and arrows indicate the direction and strength of the

587 contributions of individual variables to the principal components. Solid line represents

588 the fitted linear regression, and the gray shaded area indicates the 95% confidence

589 interval. TN: Total nitrogen; TP: Total phosphorus; MBC: Microbial biomass carbon;

590 MBN: Microbial biomass nitrogen; MBP: Microbial biomass phosphorus; BG: β-1,4-

591 glucosidase; NAG: β-1,4-N-acetylglucosaminidase; ACP: Acid phosphatase; C_{soil}:

592 Soil carbon stock. Refer to Fig. 1 for treatment details.

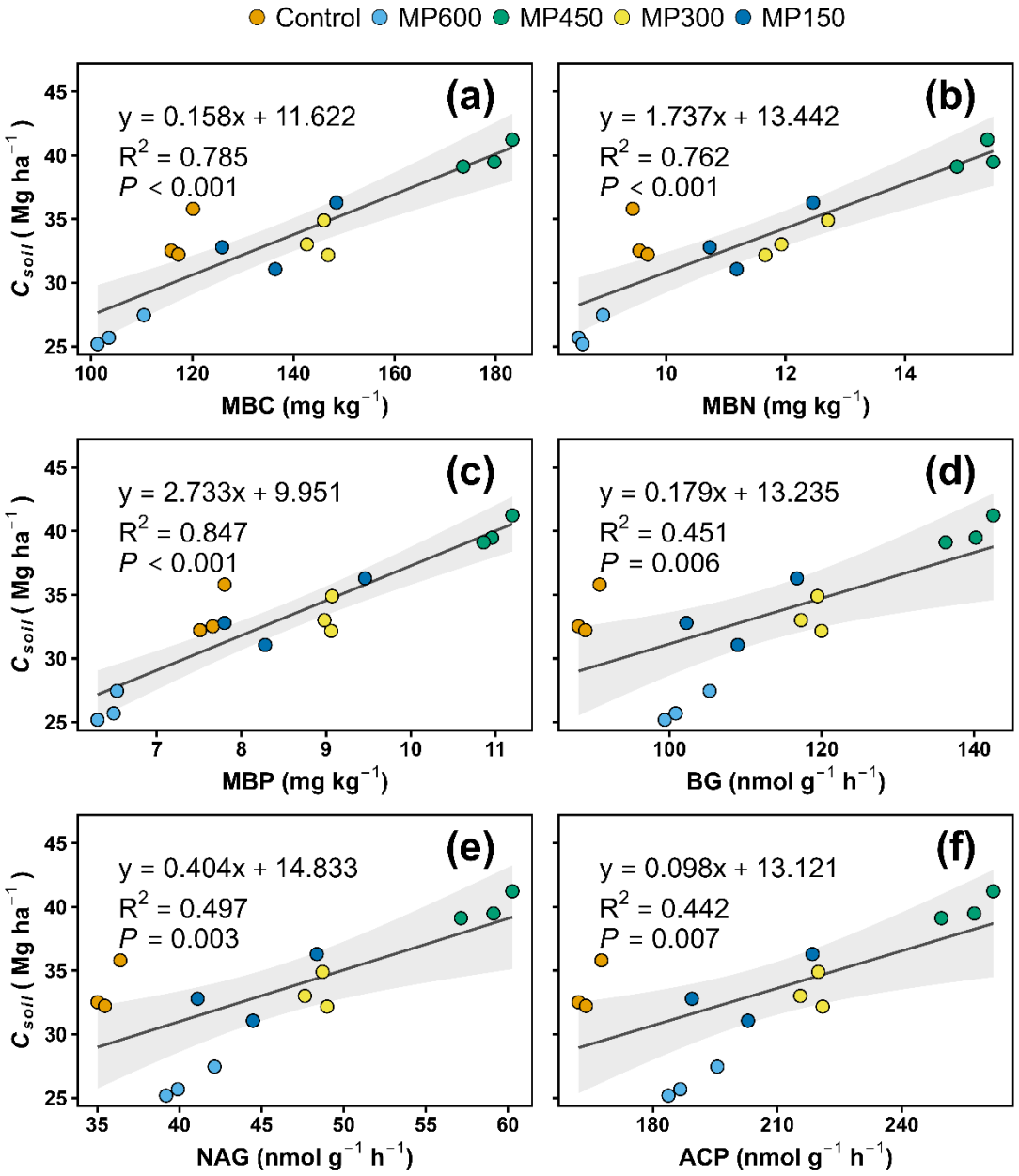

593

594 **Fig. S2** Relationships between soil carbon stock and microbial biomass and enzyme
595 activities across the five treatments. (a) Microbial biomass carbon (MBC); (b)
596 Microbial biomass nitrogen (MBN); (c) Microbial biomass phosphorus (MBP); (d) β-
597 1,4-glucosidase activity (BG); (e) β-1,4-N-acetylglucosaminidase activity (NAG); (f)
598 Acid phosphatase activity (ACP). Points indicate plot level observations. Solid lines
599 represent fitted linear regressions across all plots, and gray shaded areas indicate the

95% confidence intervals. C_{soil}: Soil carbon stock. Refer to Fig. 1 for treatment details.

4 Discussion

4.1 Structural change centered on size inequality and species mixing

TMPT altered tree size variation and species mingling more strongly than stem spatial structure. CV increased from 0.13 in the Control to 0.53–0.81 under the TMPT, while GC increased from 0.07 to 0.28–0.40 (Fig. 1a). M also increased from 0 in the Control to 0.56–0.70 under the TMPT (Fig. 1b). In contrast, W and U did not differ among treatments, and CI declined only under MP150 (Fig. 1b). Thus, six years after treatment, TMPT had increased tree size variation, size inequality, and species mixing, but had produced limited changes in the original stem spatial pattern.

The increases in CV and GC reflected the rapid formation of a two-cohort stand. Thinning retained older and larger *P. massoniana* trees, whereas mixed planting introduced a younger and smaller broadleaved cohort. This size contrast widened the diameter distribution and increased tree-size differentiation. Tree size, species composition, and stem arrangement represent distinct dimensions of mixed-stand structure and need not respond in parallel (Pommerening, 2002; Del Río et al., 2015; Ehbrecht et al., 2017; Cheng et al., 2025). Greater size differentiation can increase canopy packing and vertical resource partitioning when trees of different sizes and crown forms occupy complementary canopy space (Jucker et al., 2015; Aponte et al., 2020; Deng et al., 2025). Structural diversity has also been positively associated with forest biomass and carbon storage in other mixed forests (Fatunsin and Naka, 2025).

These studies suggest that the size differentiation observed here may create conditions for more complementary canopy use, although we did not directly measure canopy packing or light partitioning.

The increase in M reflected a direct shift from pure-pine neighborhoods to pine–broadleaved neighborhoods. M values of 0.56–0.70 indicate that the introduced broadleaved trees were already widely represented among the nearest neighbors of retained trees. Such local species mixing can change the identity and quality of litter inputs, the spatial distribution of roots, rhizosphere inputs, and local nutrient demand because conifers and broadleaved species differ in resource-acquisition strategies and tissue traits (Forrester, 2014; Dawud et al., 2016; Augusto and Boča, 2022; Lyu et al., 2023). However, the stable W and U values indicate that species introduction did not substantially change neighbor angles or local size dominance. The early structural transformation therefore arose mainly from differences in tree size and species identity, rather than from a complete reorganization of stem positions.

4.2 Larger retained pines did not offset area-based pine carbon loss

Larger retained pines did not compensate for the decline in pine carbon per unit area. As retained pine density decreased, mean individual pine biomass increased from 182 kg tree^{-1} in the Control to 280 kg tree^{-1} in MP150 (Table S2). However, C_{pine} declined from 56.86 Mg ha^{-1} in the Control to 44.64, 34.78, and 18.21 Mg ha^{-1} in MP450, MP300, and MP150, respectively (Table 1; Fig. 2). The same contrast occurred across pine organs. Individual stem biomass increased from 130 kg tree^{-1} in the Control to 199 kg tree^{-1} in MP150, whereas area-based stem carbon declined from 40.64 to 12.96

645 Mg ha^{-1} (Tables S2 and S3). Area based branch, leaf, and root carbon also declined as
646 retained pine density decreased (Tables S3-S5). Thus, the larger size of the retained
647 trees was insufficient to offset the reduction in pine stem number.
648 The larger retained pines at lower densities are consistent with competition release
649 after thinning. Lower stand density generally increases the growing space available to
650 each retained tree and reduces competition for light, water, and nutrients. These
651 changes can support wider crowns, larger diameters, and greater individual biomass
652 (Thurm and Pretzsch, 2021; Gorrod et al., 2024; Cheng et al., 2025). In our study,
653 mean DBH increased from 22.48 cm in the Control to 26.93 cm in MP150, and crown
654 width increased from 5.71 to 6.86 m (Table S2). However, thinning responses depend
655 on initial tree size, thinning intensity, species composition, and site conditions, and
656 severe thinning does not necessarily maintain stand level production (Rumpel and
657 Kögel-Knabner, 2010; Collalti et al., 2018; Thurm and Pretzsch, 2021; Gorrod et al.,
658 2024). Because pine size was measured at one time point, these differences indicate
659 larger retained trees but do not directly quantify their post treatment growth rates.
660 The divergence between individual tree size and area-based carbon reflects different
661 time scales of carbon removal and recovery. Thinning immediately removed carbon
662 stored in mature pine stems, branches, foliage, and roots, whereas carbon recovery
663 through the remaining trees accumulated gradually. Large mature trees contain
664 substantial existing carbon stocks, so their removal can reduce stand-level carbon
665 even when the retained trees subsequently benefit from lower competition (Collalti et
666 al., 2018; Zhang et al., 2018; Lázaro-Lobo et al., 2023; Yu et al., 2024). Stronger

667 thinning therefore tends to produce a larger short-term carbon deficit, although the
668 magnitude and duration of this deficit vary with thinning intensity and recovery time
669 (Jobbágy and Jackson, 2000; Zhang et al., 2024; Qu et al., 2025). In this study, area
670 based pine carbon remained the main constraint on short-term ecosystem carbon
671 under MP300 and MP150, making compensation by soil and non-pine carbon pools
672 critical to the final carbon balance.

673 **4.3 MP450 produced the most favorable short-term carbon balance**

674 MP450 produced the most favorable short-term carbon balance among the four TMPT
675 configurations. Ecosystem carbon remained comparable between MP450 and the
676 Control, at 88.48 and 92.03 Mg ha^{-1}, respectively, although MP450 contained 22%
677 less pine carbon (Fig. 2; Fig. 3; Table 1). This pine carbon loss was accompanied by
678 19% higher soil carbon, the highest understory carbon, and the highest mean
679 broadleaved carbon. Consequently, soil, broadleaved trees, understory vegetation, and
680 litter together contributed 50% of ecosystem carbon under MP450, compared with
681 38% in the Control (Fig. 2b). In contrast, MP600, MP300, and MP150 contained
682 10%, 22%, and 41% less ecosystem carbon than the Control, respectively. These
683 differences show that the short-term carbon outcome depended on how pine carbon
684 loss was balanced by soil and non-pine vegetation carbon, rather than on the response
685 of any single pool.

686 The contrast between MP600 and MP450 suggests that total post-treatment density
687 influenced this carbon balance. At treatment establishment, MP600 retained 600 pines
688 and received 300 broadleaved seedlings, producing a designed total density of 900

689 stems ha^{-1}. MP450 retained 450 pines and received the same number of broadleaved
690 seedlings, maintaining the original total density of 750 stems ha^{-1}. MP600 therefore
691 represented stand densification, whereas MP450 represented density substitution.
692 MP600 retained pine carbon near the Control level, but its soil carbon declined from
693 33.52 to 26.11 Mg ha^{-1} and its other vegetation pools remained small (Table 1). Its
694 higher total density may have maintained stronger competition for light, water, and
695 nutrients, limiting the early development of the introduced trees and understory
696 vegetation. Stand density regulates crown competition, resource capture, and growth
697 allocation, while mixture benefits depend on sufficient opportunities for resource
698 partitioning among species (Morin et al., 2011; Forrester, 2014; Thurm and Pretzsch,
699 2021; Del Río et al., 2022; Cheng et al., 2025). Because light availability and
700 belowground competition were not measured, however, these processes remain
701 possible explanations rather than directly demonstrated mechanisms.
702 MP300 and MP150 showed the opposite imbalance: stronger thinning released more
703 growing space, but their mature pine carbon losses exceeded the gains in other
704 ecosystem pools. Ecosystem carbon declined by 22% under MP300 and by 41%
705 under MP150, and the gains in soil, broadleaved, understory, and litter carbon were
706 insufficient to offset these losses (Fig. 2; Table 1). The density regressions supported
707 this interpretation. Retained pine density explained 88.5% of the variation in pine
708 carbon and 84.5% of the variation in ecosystem carbon (Fig. 4a, b). In contrast,
709 understory and litter carbon showed unimodal relationships with retained pine density,
710 with fitted maxima near 450 and 300 stems ha^{-1}, respectively (Fig. 4c, d). Moderate

711 canopy opening can support understory development, whereas litter carbon depends
712 jointly on plant inputs and decomposition conditions (Willms et al., 2017; Lei et al.,
713 2021; Lyu et al., 2023; Cheng et al., 2025). Early after thinning, stand level tree
714 carbon may therefore remain controlled mainly by retained stem number, even when
715 individual trees benefit from competition release (Collalti et al., 2018; Zhang et al.,
716 2018; Gong et al., 2021; Zhang et al., 2024).
717 Soil and broadleaved carbon did not follow retained pine density, indicating that
718 carbon pools responded to different parts of the post treatment environment. Neither
719 C_{soil} nor $C_{broadleaf}$ was significantly related to retained pine density (Fig. S1). Soil
720 carbon depends on organic inputs, soil conditions, and microbial processing, while
721 broadleaved carbon depends on species identity, establishment, and interactions with
722 the residual pine layer. These controls extend beyond retained pine stem number alone
723 (Forrester, 2014; Augusto and Boča, 2022; Bryant et al., 2024; Sullivan et al., 2025;
724 Zhang et al., 2026). The positive broadleaved carbon values under all TMPT confirm
725 the establishment of the introduced cohort, but they do not test whether the mixtures
726 produced more broadleaved carbon than broadleaved monocultures.
727 Mixed planting therefore did not provide a uniform ecosystem carbon benefit across
728 thinning intensities. A mixed *Castanopsis hystrix–P. massoniana* plantation in
729 Guangxi stored more ecosystem carbon than a pure *P. massoniana* plantation, whereas
730 spruce–birch mixtures changed carbon allocation without exceeding spruce
731 monocultures in total ecosystem carbon (He et al., 2013; Täll et al., 2025). Broader
732 comparisons similarly show that mixed plantations do not always exceed

monocultures in biomass, multifunctionality, or ecosystem carbon because outcomes depend on species identity, stand density, stand age, and soil conditions (Augusto and Boča, 2022; Li et al., 2024; Zhang et al., 2026). MP450 should therefore be interpreted as the most favorable short-term configuration among the treatments tested, rather than as evidence that mixed planting universally increases ecosystem carbon. Its advantage was that it maintained total carbon across ecosystem pools, not that every carbon pool increased simultaneously. This pool-based interpretation is consistent with an ecosystem-level view of forest carbon, in which carbon allocation among components matters alongside total storage (Pugh et al., 2019; Heinrich et al., 2023; Pan et al., 2024).

4.4 Soil carbon covaried with nutrient microbial conditions

The higher soil carbon under MP450 coincided with coordinated changes in soil nutrients, physical conditions, microbial biomass, and enzyme activities. Compared with the Control, MP450 increased soil carbon stock by 19% and SOC concentration by 38% (Table 1; Table 2). MP450 also increased TN by 25%, raised pH from 4.25 to 4.40, and reduced SBD from 1.29 to 1.12 g cm^{-3} (Fig. 5; Table 2). Microbial biomass showed similarly strong responses: MBC, MBN, and MBP were 52%, 59%, and 44% higher than in the Control, respectively. BG, NAG, and ACP activities also increased by 56%–65%. These parallel responses indicate that the higher soil carbon under MP450 formed part of a broader change in the surface-soil environment rather than a response to retained pine density alone.

The modest increase in pH and the higher nutrient concentrations may reflect changes in plant inputs after reducing pine dominance and introducing broadleaved species. Broadleaved litter often returns more base cations and nutrients than pine needles, which can partly buffer soil acidity and alter nutrient availability during decomposition (Dawud et al., 2016; Cruz-Paredes et al., 2021; Lei et al., 2021; Xu et al., 2024; Lin et al., 2025). However, the 0.15-unit pH increase was small and should not be treated as a complete reversal of soil acidification. The concurrent increases in TP and ACP suggest greater phosphorus turnover under MP450. Root exudates can mobilize phosphorus through organic acid release and ligand exchange, while greater microbial demand can stimulate phosphatase production and organic phosphorus mineralization (Richardson et al., 2009; Wu et al., 2023; Qu et al., 2025). Because available phosphorus, root exudates, and different inorganic and organic phosphorus fractions were not measured, the present data cannot distinguish among these pathways.

The parallel increases in microbial biomass and C, N, and P-acquiring enzymes indicate stronger microbial processing under MP450. MBC, MBN, and MBP represent the active microbial pools of carbon, nitrogen, and phosphorus. BG supports microbial acquisition of carbon from cellulose derived compounds, NAG contributes to nitrogen acquisition from chitin, and ACP releases phosphate from organic compounds. Their concurrent increases therefore indicate a broad microbial response rather than a change restricted to one nutrient cycle (Sinsabaugh et al., 2008; Burns et al., 2013; Xu et al., 2022). Greater vegetation inputs may have supplied substrates for

776 this response. MP450 increased understory carbon from 1.00 to 1.56 Mg ha^{-1}, and also
777 contained the highest mean broadleaved carbon (Table 1). Understory vegetation and
778 broadleaved trees can contribute litter, fine roots, and rhizosphere carbon, while lower
779 bulk density may improve root penetration and soil aeration. Litter quality, root
780 inputs, belowground biomass, and soil physical conditions are important controls on
781 SOC formation in mixed and subtropical forests (Cotrufo et al., 2013; Dawud et al.,
782 2016; Lin et al., 2025).
783 The association between C_{soil} and the soil nutrient–microbial axis supports
784 coordinated change but does not identify the process that retained carbon. PC1
785 explained 82.0% of the variation in pH, TN, TP, microbial biomass, and enzyme
786 activities, and standardized PC1 scores explained 62.4% of the variation in C_{soil} (Fig.
787 6a, b). C_{soil} was also positively related to MBC, MBN, MBP, BG, NAG, and ACP in
788 the separate regressions (Fig. S2). These relationships demonstrate covariation rather
789 than causation. Greater enzyme activity can accelerate organic matter decomposition
790 as well as the microbial transformation of plant inputs, so its positive relationship with
791 C_{soil} does not by itself demonstrate soil carbon stabilization. Greater microbial
792 biomass could contribute to longer-term carbon formation through microbial residues
793 and mineral associated organic matter, but this pathway requires direct measurements
794 of microbial necromass and soil carbon fractions (Cotrufo et al., 2013; Liang et al.,
795 2017; Zhou et al., 2020; Lei et al., 2021; Xu et al., 2024).
796 The non-monotonic soil response further shows that an intermediate stand
797 configuration, rather than retained pine density alone, favored the observed soil

conditions. MP600 maintained the highest total post treatment density but had the lowest SOC, MBC, MBN, and MBP among the TMPT. MP300 and MP150 released more growing space than MP450, but neither reached the SOC, microbial biomass, or enzyme activity levels observed under MP450 (Table 2). MP450 may therefore have combined sufficient canopy opening and vegetation inputs with enough overstory retention to maintain belowground carbon supply. Similar studies show that soil responses to thinning and species mixing depend on treatment intensity, recovery time, species traits, and initial soil conditions (Gong et al., 2021; Xu et al., 2024; Qu et al., 2025). This interpretation remains provisional because the study did not directly quantify light, litter production, root turnover, or rhizosphere carbon inputs.

4.5 Management implications

Plantation transformation should balance the retention of existing pine carbon with the growing space needed by introduced broadleaved trees and understory vegetation. In this study, MP600 retained pine carbon near the Control level but did not maintain ecosystem carbon, suggesting that adding broadleaved trees without enough pine removal may intensify competition and limit early gains in other pools. MP300 and MP150 released more growing space, but their pine carbon losses were too large to be offset within six years. MP450 provided the most favorable short-term balance among the tested configurations: its designed post treatment density remained equal to the original 750 stems ha^{-1}, ecosystem carbon remained near the Control, and soil and non-pine vegetation carbon were higher. Density substitution may therefore provide a useful operational approach for transforming similar *P. massoniana* plantations

without substantially increasing total stem density or causing excessive short-term carbon loss. This result should be interpreted as a short-term, site, and species-specific finding rather than as a universal optimum of 450 retained pine stems ha^{-1}; long-term monitoring is still needed to test whether this balance persists as the introduced broadleaved trees mature.

5 Conclusions

Six years after thinning and mixed planting, TMPT reallocated carbon among ecosystem pools rather than producing a uniform increase in ecosystem carbon. The treatments increased tree size variation, size inequality, and species mingling, but changed most dimensions of stem spatial structure only weakly. Retained pines were larger at lower densities, yet greater individual biomass did not compensate for the decline in pine carbon per unit area. Stronger thinning under MP300 and MP150 therefore reduced ecosystem carbon, whereas MP450 maintained ecosystem carbon near the unthinned Control. MP450 achieved this balance because its moderate pine carbon loss was accompanied by higher soil carbon and greater carbon in non-pine vegetation. Retained pine density explained pine and ecosystem carbon but did not explain soil or broadleaved carbon. Soil carbon instead covaried with soil nutrients, microbial biomass, and C, N, and P acquiring enzyme activities. Among the configurations tested, density substitution under MP450 provided the most favorable short-term balance between retaining mature pine carbon and developing other ecosystem carbon pools. Long-term monitoring is required to determine whether this

balance persists as the introduced broadleaved trees mature and stand competition changes.

CRediT authorship contribution statement

Zeyao Zhao: Writing – review & editing, Supervision, Methodology, Formal analysis, Data curation, Conceptualization. Ning An: Methodology, Investigation, Formal analysis, Resources. Wenjun Xie: Investigation, Formal analysis, Data curation. Nan Jiang: Investigation, Formal analysis. Zhaogui Yan: Writing – review & editing, Writing – original draft, Visualization, Validation, Supervision, Resources. Li Mei: Writing – review & editing, Validation, Supervision, Resources, Project administration, Methodology, Funding acquisition, Formal analysis, Conceptualization.

Declaration of competing interests

In submitting this manuscript, we provide the following statements: (1) No conflict of interest exists in the submission of this manuscript; (2) The manuscript is approved by all authors; (3) The work described was original and has not been published previously, and is not under consideration for publication elsewhere; (4) All the authors listed have made substantial contributions to the research design, or the acquisition, analysis or interpretation of data, or drafting the paper or revising it critically; and (5) Nobody who qualifies for authorship has been excluded.

Acknowledgements

This study was supported by National Key Research and Development Program of China (Grant Nos. 2023YFD2200902-01 and 2023YFD2200902-04). We thank the

members of the Hubei Engineering Technology Research Center for Forestry Information and the Experimental Center of Tropical Forestry for their invaluable assistance.

Data availability

Data will be made available on request.

References

Ali, A., Lin, S.-L., He, J.-K., Kong, F.-M., Yu, J.-H., Jiang, H.-S. 2019. Climate and soils determine aboveground biomass indirectly via species diversity and stand structural complexity in tropical forests. Forest Ecology and Management 432: 823-831. https://doi.org/10.1016/j.foreco.2018.10.024.

Ammer, C. 2018. Diversity and forest productivity in a changing climate. New Phytologist 221: 50-66. https://doi.org/10.1111/nph.15263.

Aponte, C., Kasel, S., Nitschke, C.R., Tanase, M.A., Vickers, H., Parker, L., Fedrigo, M., Kohout, M., Ruiz-Benito, P., Zavala, M.A., Bennett, L.T., Hickler, T. 2020. Structural diversity underpins carbon storage in Australian temperate forests. Global Ecology and Biogeography 29: 789-802. https://doi.org/10.1111/geb.13038.

Augusto, L., Boča, A. 2022. Tree functional traits, forest biomass, and tree species diversity interact with site properties to drive forest soil carbon. Nature Communications 13. https://doi.org/10.1038/s41467-022-28748-0.

Bao, S., 2000. Tu rang nong hua fen xi [Soil agrochemical analysis]. China Agriculture Press.

Brancalion, P.H.S., Holl, K.D. 2020. Guidance for successful tree planting initiatives. Journal of Applied Ecology 57: 2349-2361. https://doi.org/10.1111/1365-2664.13725.

Bryant, R.L., Kothari, S., Cavender-Bares, J., Curran, S.J., Grossman, J.J., Hobbie, S.E., Nash, C., Neumiller, G.C., See, C.R. 2024. Independent effects of tree diversity on aboveground and soil carbon pools after six years of experimental afforestation. Ecological Applications 34. https://doi.org/10.1002/eap.3042.

Burns, R.G., DeForest, J.L., Marxsen, J., Sinsabaugh, R.L., Stromberger, M.E., Wallenstein, M.D.,

Weintraub, M.N., Zoppini, A. 2013. Soil enzymes in a changing environment: Current knowledge and future directions. Soil Biology and Biochemistry 58: 216-234. https://doi.org/10.1016/j.soilbio.2012.11.009.

Che, Y., Cai, H., Jin, G. 2024. Scale-dependent effects of vegetation attributes and soil fertility on productivity in two temperate forests in Northeast China. Catena 245. https://doi.org/10.1016/j.catena.2024.108331.

Cheng, F., Zhao, X., Luo, Y., Tian, J., Sun, Y., Wang, H., Wang, Q., Zhu, J., Yang, C., He, H., Liu, G. 2025. Effects of thinning on canopy structure, forest productivity, and productivity stability in mixed conifer-broadleaf forest: Insights from a LiDAR survey. Journal of Environmental Management 385. https://doi.org/10.1016/j.jenvman.2025.125707.

Collalti, A., Trotta, C., Keenan, T.F., Ibrom, A., Bond-Lamberty, B., Grote, R., Vicca, S., Reyer, C.P.O., Migliavacca, M., Veroustraete, F., Anav, A., Campioli, M., Scoccimarro, E., Šigut, L., Grieco, E., Cescatti, A., Matteucci, G. 2018. Thinning Can Reduce Losses in Carbon Use Efficiency and Carbon Stocks in Managed Forests Under Warmer Climate. Journal of Advances in Modeling Earth Systems 10: 2427-2452. https://doi.org/10.1029/2018ms001275.

Cotrufo, M.F., Wallenstein, M.D., Boot, C.M., Denef, K., Paul, E. 2013. The Microbial Efficiency-Matrix Stabilization (MEMS) framework integrates plant litter decomposition with soil organic matter stabilization: do labile plant inputs form stable soil organic matter? Global Change Biology 19: 988-995. https://doi.org/10.1111/gcb.12113.

Cruz-Paredes, C., Diera, T., Davey, M., Rieckmann, M.M., Christensen, P., Dela Cruz, M., Laursen, K.H., Joner, E.J., Christensen, J.H., Nybroe, O., Jakobsen, I. 2021. Disentangling the abiotic and biotic components of AMF suppressive soils. Soil Biology and Biochemistry 159. https://doi.org/10.1016/j.soilbio.2021.108305.

Dawud, S.M., Raulund-Rasmussen, K., Domisch, T., Finér, L., Jaroszewicz, B., Vesterdal, L. 2016. Is Tree Species Diversity or Species Identity the More Important Driver of Soil Carbon Stocks, C/N Ratio, and pH? Ecosystems 19: 645-660. https://doi.org/10.1007/s10021-016-9958-1.

De Mendiburu, F., Simon, R. 2015. Agricolae - Ten years of an open source statistical tool for experiments in breeding, agriculture and biology. PeerJ PrePrints.

https://doi.org/10.7287/peerj.preprints.1404v1.

Del Río, M., Pretzsch, H., Alberdi, I., Bielak, K., Bravo, F., Brunner, A., Condés, S., Ducey, M.J., Fonseca, T., von Lüpke, N., Pach, M., Peric, S., Perot, T., Souidi, Z., Spathelf, P., Sterba, H., Tijardovic, M., Tomé, M., Vallet, P., Bravo-Oviedo, A. 2015. Characterization of the structure, dynamics, and productivity of mixed-species stands: review and perspectives. European Journal of Forest Research 135: 23-49. https://doi.org/10.1007/s10342-015-0927-6.

Del Río, M., Pretzsch, H., Ruiz-Peinado, R., Jactel, H., Coll, L., Löf, M., Aldea, J., Ammer, C., Avdagić, A., Barbeito, I., Bielak, K., Bravo, F., Brazaitis, G., Cerný, J., Collet, C., Condés, S., Drössler, L., Fabrika, M., Heym, M., Holm, S.O., Hylen, G., Jansons, A., Kurylyak, V., Lombardi, F., Matović, B., Metslaid, M., Motta, R., Nord-Larsen, T., Nothdurft, A., den Ouden, J., Pach, M., Pardos, M., Poeydebat, C., Ponette, Q., Pérot, T., Reventlow, D.O.J., Sitko, R., Sramek, V., Steckel, M., Svoboda, M., Verheyen, K., Vospernik, S., Wolff, B., Zlatanov, T., Bravo-Oviedo, A. 2022. Emerging stability of forest productivity by mixing two species buffers temperature destabilizing effect. Journal of Applied Ecology 59: 2730-2741. https://doi.org/10.1111/1365-2664.14267.

Deng, X., Schmid, B., Bruelheide, H., Chen, C., Li, Y., Li, S., Morsdorf, F., Ray, T., Schuman, M.C., Tang, T., von Oheimb, G., Ma, K., Liu, X. 2025. Forest biodiversity increases productivity via complementarity from greater canopy structural complexity. Proceedings of the National Academy of Sciences 122. https://doi.org/10.1073/pnas.2506750122.

Dixon, R.K., Solomon, A.M., Brown, S., Houghton, R.A., Trexier, M.C., Wisniewski, J. 1994. Carbon Pools and Flux of Global Forest Ecosystems. Science 263: 185-190. https://doi.org/10.1126/science.263.5144.185.

Dong, L., Bettinger, P., Liu, Z. 2022. Optimizing neighborhood-based stand spatial structure: Four cases of boreal forests. Forest Ecology and Management 506. https://doi.org/10.1016/j.foreco.2021.119965.

Ehbrecht, M., Schall, P., Ammer, C., Seidel, D. 2017. Quantifying stand structural complexity and its relationship with forest management, tree species diversity and microclimate. Agricultural and Forest Meteorology 242: 1-9. https://doi.org/10.1016/j.agrformet.2017.04.012.

Fatunsin, O.E., Naka, K. 2025. Structural diversity enhances carbon storage in mixed oak-pine forests of the Southeast United States. Forest Ecology and Management 586. https://doi.org/10.1016/j.foreco.2025.122719.

Forrester, D.I. 2014. The spatial and temporal dynamics of species interactions in mixed-species forests: From pattern to process. Forest Ecology and Management 312: 282-292. https://doi.org/10.1016/j.foreco.2013.10.003.

Gardner, C.J., Bicknell, J.E., Baldwin-Cantello, W., Struebig, M.J., Davies, Z.G. 2019. Quantifying the impacts of defaunation on natural forest regeneration in a global meta-analysis. Nature Communications 10: 4590. https://doi.org/10.1038/s41467-019-12539-1.

Gong, C., Tan, Q., Liu, G., Xu, M. 2021. Forest thinning increases soil carbon stocks in China. Forest Ecology and Management 482. https://doi.org/10.1016/j.foreco.2020.118812.

Gorrod, E., White, L., Bedward, M., Hope, B., Chu, N., McAllister, D. 2024. Restoration thinning accelerates small tree growth but may slow large tree growth in a multi-age flood-dependent forest. Journal of Applied Ecology 61: 1560–1572. https://doi.org/10.1111/1365-2664.14668.

Han, X., Ali, I., Ullah, S., Zhang, Y., Xu, Y., Yang, M. 2025. Ecological benefits of integrating broadleaf tree species into *Pinus massoniana* monocultures and their impacts on soil fertility microbial diversity and network stability. Forest Ecology and Management 586. https://doi.org/10.1016/j.foreco.2025.122712.

He, Y., Jiang, C., Fan, R., Lan, Y., Zhang, H., Cui, Y., Li, L., Wu, H., Ye, S. 2024. Mixed Eucalyptus plantations enhance soil organic carbon accumulation and chemical stability through soil microbial community and multifunctionality. Catena 245. https://doi.org/10.1016/j.catena.2024.108315.

He, Y., Qin, L., Li, Z., Liang, X., Shao, M., Tan, L. 2013. Carbon storage capacity of monoculture and mixed-species plantations in subtropical China. Forest Ecology and Management 295: 193-198. https://doi.org/10.1016/j.foreco.2013.01.020.

Hedges, L.V. 1981. Distribution Theory for Glass's Estimator of Effect size and Related Estimators. Journal of Educational Statistics 6: 107-128. https://doi.org/10.3102/10769986006002107.

Heinrich, V.H.A., Vancutsem, C., Dalagnol, R., Rosan, T.M., Fawcett, D., Silva-Junior, C.H.L.,

Cassol, H.L.G., Achard, F., Jucker, T., Silva, C.A., House, J., Sitch, S., Hales, T.C., Aragão, L.E.O.C. 2023. The carbon sink of secondary and degraded humid tropical forests. Nature 615: 436-442. https://doi.org/10.1038/s41586-022-05679-w.

http://www.nmc.cn/ (accessed 9 May 2026).

Jobbágy, E.G., Jackson, R.B. 2000. The Vertical Distribution of Soil Organic Carbon and Its Relation To Climate and Vegetation. Ecological Applications 10: 423-436. https://doi.org/10.1890/1051-0761(2000)010[0423:Tvdoso]2.0.Co;2.

Joshi, R.K., Garkoti, S.C. 2023. Influence of vegetation types on soil physical and chemical properties, microbial biomass and stoichiometry in the central Himalaya. Catena 222. https://doi.org/10.1016/j.catena.2022.106835.

Jucker, T., Bouriaud, O., Coomes, D.A., Baltzer, J. 2015. Crown plasticity enables trees to optimize canopy packing in mixed-species forests. Functional Ecology 29: 1078-1086. https://doi.org/10.1111/1365-2435.12428.

Keenan, T.F., Prentice, I.C., Canadell, J.G., Williams, C.A., Wang, H., Raupach, M., Collatz, G.J. 2016. Recent pause in the growth rate of atmospheric CO2 due to enhanced terrestrial carbon uptake. Nature Communications 7. https://doi.org/10.1038/ncomms13428.

Lázaro-Lobo, A., Ruiz-Benito, P., Cruz-Alonso, V., Castro-Díez, P. 2023. Quantifying carbon storage and sequestration by native and non-native forests under contrasting climate types. Global Change Biology 29: 4530-4542. https://doi.org/10.1111/gcb.16810.

Lei, L., Xiao, W., Zeng, L., Frey, B., Huang, Z., Zhu, J., Cheng, R., Li, M.-H. 2021. Effects of thinning intensity and understory removal on soil microbial community in Pinus massoniana plantations of subtropical China. Applied Soil Ecology 167. https://doi.org/10.1016/j.apsoil.2021.104055.

Leverkus, A.B., Polo, I., Baudoux, C., Thorn, S., Gustafsson, L., Rubio de Casas, R., Bogdziewicz, M. 2021. Resilience impacts of a secondary disturbance: Meta-analysis of salvage logging effects on tree regeneration. Journal of Ecology 109: 3224-3232. https://doi.org/10.1111/1365-2745.13581.

Li, X., Liu, Y., Wu, G., Lie, Z., Sheng, H., Aguila, L.C.R., Khan, M.S., Liu, X., Zhou, S., Wu, T., Xu, W., Liu, J. 2024. Mixed plantations do not necessarily provide higher ecosystem multifunctionality than monoculture plantations. Science of The Total Environment 914.

https://doi.org/10.1016/j.scitotenv.2024.170156.

Li, Y., Fang, X., Xiang, W., Lei, P., Chen, L., Ouyang, S., Deng, X., Hu, Y., Wu, H. 2026. Species identity outweighs richness in shaping soil microbial resource limitation in subtropical mixed *Pinus massoniana*-broadleaved plantations. Catena 264. https://doi.org/10.1016/j.catena.2025.109744.

Liang, C., Schimel, J.P., Jastrow, J.D. 2017. The importance of anabolism in microbial control over soil carbon storage. Nature Microbiology 2. https://doi.org/10.1038/nmicrobiol.2017.105.

Liang, J., Crowther, T.W., Picard, N., Wiser, S., Zhou, M., Alberti, G., Schulze, E.-D., McGuire, A.D., Bozzato, F., Pretzsch, H., de-Miguel, S., Paquette, A., Hérault, B., Scherer-Lorenzen, M., Barrett, C.B., Glick, H.B., Hengeveld, G.M., Nabuurs, G.-J., Pfautsch, S., Viana, H., Vibrans, A.C., Ammer, C., Schall, P., Verbyla, D., Tchebakova, N., Fischer, M., Watson, J.V., Chen, H.Y.H., Lei, X., Schelhaas, M.-J., Lu, H., Gianelle, D., Parfenova, E.I., Salas, C., Lee, E., Lee, B., Kim, H.S., Bruelheide, H., Coomes, D.A., Piotto, D., Sunderland, T., Schmid, B., Gourlet-Fleury, S., Sonké, B., Tavani, R., Zhu, J., Brandl, S., Vayreda, J., Kitahara, F., Searle, E.B., Neldner, V.J., Ngugi, M.R., Baraloto, C., Frizzera, L., Bałazy, R., Oleksyn, J., Zawiła-Niedźwiecki, T., Bouriaud, O., Bussotti, F., Finér, L., Jaroszewicz, B., Jucker, T., Valladares, F., Jagodzinski, A.M., Peri, P.L., Gonmadje, C., Marthy, W., O'Brien, T., Martin, E.H., Marshall, A.R., Rovero, F., Bitariho, R., Niklaus, P.A., Alvarez-Loayza, P., Chamuya, N., Valencia, R., Mortier, F., Wortel, V., Engone-Obiang, N.L., Ferreira, L.V., Odeke, D.E., Vasquez, R.M., Lewis, S.L., Reich, P.B. 2016. Positive biodiversity-productivity relationship predominant in global forests. Science 354. https://doi.org/10.1126/science.aaf8957.

Liang, Z., Wang, X., Li, Y., Ma, X., Li, Y., Li, L., Dong, W., Sheng, Q., Wang, W. 2025. Structural diversity enhances the temporal effects of thinning on carbon storage in pine-oak mixed forests. Environ Manage 381: 125304. https://doi.org/10.1016/j.jenvman.2025.125304.

Lin, H., He, Z., Tian, K., Kong, X., Li, Z., Zhou, F., Tian, X. 2025. Factors influencing soil carbon stocks in secondary subtropical forests of eastern China. Catena 260. https://doi.org/10.1016/j.catena.2025.109419.

Liu, Y., Li, Q., Tian, H., Liu, S., Ma, C., Wang, M., Wang, H., Ming, A. 2025. Nitrogen-fixing tree

species enhance the positive effects of tree species richness on soil organic carbon sequestration by increasing fine root phosphorus loss. Catena 254. https://doi.org/10.1016/j.catena.2025.108927.

Luo, Y.-J., Wang, X.-K., Ouyang, Z.-Y., Lu, F., Feng, L.-G., Tao, J. 2020. A review of biomass equations for China's tree species. Earth System Science Data 12: 21-40. https://doi.org/10.5194/essd-12-21-2020.

Lyu, M., Homyak, P.M., Xie, J., Peñuelas, J., Ryan, M.G., Xiong, X., Sardans, J., Lin, W., Wang, M., Chen, G., Yang, Y. 2023. Litter quality controls tradeoffs in soil carbon decomposition and replenishment in a subtropical forest. Journal of Ecology 111: 2181-2193. https://doi.org/10.1111/1365-2745.14167.

Miao, Y.Z., Tong, R., Zhu, N., Chen, S., Zhou, F., Wang, G.G., Wu, T. 2025. Effects of stand structural diversity on carbon storage of Masson pine forests in Fengyang Mountain Nature Reserve, China. Forestry Research e011. https://doi.org/10.48130/forres-0025-0010.

Moraes, L.M., de Azevedo, J.C., Filho, N.M.L., de Oliveira, J.V.C., Abreu, N.L., Ruggieri, A.C., de Souza Bahia, A.S.R., da Silva Cardoso, A., Carneiro e Pedreira, B., Costa, V.E., da Silva, T.C., Faturi, C., do Rêgo, A.C. 2026. How do land use changes affect carbon and nitrogen stocks in Amazon soils under different climatic types? Catena 268. https://doi.org/10.1016/j.catena.2026.110065.

Morin, X., Fahse, L., Scherer-Lorenzen, M., Bugmann, H. 2011. Tree species richness promotes productivity in temperate forests through strong complementarity between species. Ecology Letters 14: 1211-1219. https://doi.org/10.1111/j.1461-0248.2011.01691.x.

Osei, R., Titeux, H., Bielak, K., Bravo, F., Collet, C., Cools, C., Cornelis, J.-T., Heym, M., Korboulewsky, N., Löf, M., Muys, B., Najib, Y., Nothdurft, A., Pach, M., Pretzsch, H., del Rio, M., Ruiz-Peinado, R., Ponette, Q. 2021. Tree species identity drives soil organic carbon storage more than species mixing in major two-species mixtures (pine, oak, beech) in Europe. Forest Ecology and Management 481. https://doi.org/10.1016/j.foreco.2020.118752.

Pan, Y., Birdsey, R.A., Phillips, O.L., Houghton, R.A., Fang, J., Kauppi, P.E., Keith, H., Kurz, W.A., Ito, A., Lewis, S.L., Nabuurs, G.-J., Shvidenko, A., Hashimoto, S., Lerink, B.,

Schepaschenko, D., Castanho, A., Murdiyarso, D. 2024. The enduring world forest carbon sink. Nature 631: 563-569. https://doi.org/10.1038/s41586-024-07602-x.

Pan, Y., Birdsey, R.A., Fang, J., Houghton, R., Kauppi, P.E., Kurz, W.A., Phillips, O.L., Shvidenko, A., Lewis, S.L., Canadell, J.G., Ciais, P., Jackson, R.B., Pacala, S.W., McGuire, A.D., Piao, S., Rautiainen, A., Sitch, S., Hayes, D. 2011. A large and persistent carbon sink in the world's forests. Science 333: 988-993. https://doi.org/10.1126/science.1201609.

Paquette, A., Messier, C. 2010. The effect of biodiversity on tree productivity: from temperate to boreal forests. Global Ecology and Biogeography 20: 170-180. https://doi.org/10.1111/j.1466-8238.2010.00592.x.

Pommerening, A. 2002. Approaches to quantifying forest structures. Forestry 75: 305–324. https://doi.org/10.1093/forestry/75.3.305.

Pugh, T.A.M., Lindeskog, M., Smith, B., Poulter, B., Arneth, A., Haverd, V., Calle, L. 2019. Role of forest regrowth in global carbon sink dynamics. Proceedings of the National Academy of Sciences 116: 4382-4387. https://doi.org/10.1073/pnas.1810512116.

Qi, D., Feng, F., Lu, C., Fu, Y. 2022. C:N:P stoichiometry of different soil components after the transition of temperate primary coniferous and broad-leaved mixed forests to secondary forests. Soil and Tillage Research 216. https://doi.org/10.1016/j.still.2021.105260.

Qin, Y., He, X., Lei, X., Feng, L., Zhou, Z., Lu, J. 2022. Tree size inequality and competition effects on nonlinear mixed effects crown width model for natural spruce-fir-broadleaf mixed forest in northeast China. Forest Ecology and Management 518. https://doi.org/10.1016/j.foreco.2022.120291.

Qu, Q., Xu, H., Xu, L., You, C., Tan, B., Li, H., Zhang, L., Wang, L., Liu, S., Xu, Z., Xue, S., Wang, M. 2025. Forest thinning effects on soil carbon stocks and dynamics: Perspective of soil organic carbon sequestration rates. Catena 250. https://doi.org/10.1016/j.catena.2025.108759.

R Core Team. 2024. R: A language and environment for statistical computing. R Foundation for Statistical Computing, Vienna, Austria. https://doi.org/10.32614/R.manuals.

Richardson, A.E., Barea, J.-M., McNeill, A.M., Prigent-Combaret, C. 2009. Acquisition of phosphorus and nitrogen in the rhizosphere and plant growth promotion by

1100 microorganisms. Plant and Soil 321: 305-339. https://doi.org/10.1007/s11104-009-9895-
1101 2.
1102 Rumpel, C., Kögel-Knabner, I. 2010. Deep soil organic matter—a key but poorly understood
1103 component of terrestrial C cycle. Plant and Soil 338: 143-158.
1104 https://doi.org/10.1007/s11104-010-0391-5.
1105 Sandra, P.R., Shankar, A., Garkoti, S.C., Adarsh, C.K. 2025. Understanding the effects of forest
1106 types, vegetation structural diversity, and soil properties on above- and below-ground
1107 carbon stock of moist deciduous forest ecosystems in Western Ghats, India. Catena 257.
1108 https://doi.org/10.1016/j.catena.2025.109198.
1109 Sinsabaugh, R.L., Lauber, C.L., Weintraub, M.N., Ahmed, B., Allison, S.D., Crenshaw, C.,
1110 Contosta, A.R., Cusack, D., Frey, S., Gallo, M.E., Gartner, T.B., Hobbie, S.E., Holland,
1111 K., Keeler, B.L., Powers, J.S., Stursova, M., Takacs-Vesbach, C., Waldrop, M.P.,
1112 Wallenstein, M.D., Zak, D.R., Zeglin, L.H. 2008. Stoichiometry of soil enzyme activity at
1113 global scale. Ecology Letters 11: 1252-1264. https://doi.org/10.1111/j.1461-
1114 0248.2008.01245.x.
1115 Sullivan, T.P., Sullivan, D.S., Lindgren, P.M.F., Ransome, D.B., Sullivan, J.H.-r. 2025. Thirty-year
1116 responses of ecosystem components to stand thinning in lodgepole pine forest: Old-forest
1117 attributes, stand structure, and forest-floor small mammals. Forest Ecology and
1118 Management 587. https://doi.org/10.1016/j.foreco.2025.122733.
1119 Täll, K., Tullus, A., Tullus, T., Tullus, H., Lutter, R. 2025. Ecosystem carbon storage two decades
1120 after afforestation in Norway spruce and silver birch monocultures and mixtures on
1121 abandoned agricultural land in hemiboreal Estonia. Forest Ecology and Management 578.
1122 https://doi.org/10.1016/j.foreco.2024.122444.
1123 Thurm, E.A., Pretzsch, H. 2021. Growth–density relationship in mixed stands – Results from
1124 long-term experimental plots. Forest Ecology and Management 483.
1125 https://doi.org/10.1016/j.foreco.2020.118909.
1126 Willms, J., Bartuszevige, A., Schwilk, D.W., Kennedy, P.L. 2017. The effects of thinning and
1127 burning on understory vegetation in North America: A meta-analysis. Forest Ecology and
1128 Management 392: 184-194. https://doi.org/10.1016/j.foreco.2017.03.010.
1129 Wu, L., Zou, B., Wang, S., Zhou, L., Zheng, Y., Huang, Z., He, J.-Z. 2023. Effects of multispecies

restoration on soil extracellular enzyme activity stoichiometry in Pinus massoniana plantations of subtropical China. Soil Biology and Biochemistry 178. https://doi.org/10.1016/j.soilbio.2023.108967.

Xu, H., Gan, Q., Huang, L., Pan, X., Liu, T., Wang, R., Wang, L., Zhang, L., Li, H., Wang, L., Liu, S., Li, J., You, C., Xu, L., Tan, B., Xu, Z. 2024. Effects of forest thinning on soil microbial biomass and enzyme activity. Catena 239. https://doi.org/10.1016/j.catena.2024.107938.

Xu, M., Liu, H., Zhang, Q., Zhang, Z., Ren, C., Feng, Y., Yang, G., Han, X., Zhang, W. 2022. Effect of forest thinning on soil organic carbon stocks from the perspective of carbon-degrading enzymes. Catena 218. https://doi.org/10.1016/j.catena.2022.106560.

Yu, Z., Liu, S., Li, H., Liang, J., Liu, W., Piao, S., Tian, H., Zhou, G., Lu, C., You, W., Sun, P., Dong, Y., Sitch, S., Agathokleous, E. 2024. Maximizing carbon sequestration potential in Chinese forests through optimal management. Nature Communications 15. https://doi.org/10.1038/s41467-024-47143-5.

Zhang, H., Feng, H., Qu, X., Yang, M., Huang, M., Jacobs, D.F., Guo, J. 2026. Species mixing promotes plant biomass accumulation and nutrient cycling in forest plantations. Communications Biology 9. https://doi.org/10.1038/s42003-026-09646-3.

Zhang, H., Liu, S., Yu, J., Li, J., Shangguan, Z., Deng, L. 2024. Thinning increases forest ecosystem carbon stocks. Forest Ecology and Management 555. https://doi.org/10.1016/j.foreco.2024.121702.

Zhang, X., Guan, D., Li, W., Sun, D., Jin, C., Yuan, F., Wang, A., Wu, J. 2018. The effects of forest thinning on soil carbon stocks and dynamics: A meta-analysis. Forest Ecology and Management 429: 36-43. https://doi.org/10.1016/j.foreco.2018.06.027.

Zhang, Y., Zhao, D., Lin, J., Jiang, L., Huang, B., Jiang, F., Wang, M.-K., Ge, H., Huang, Y. 2020. Impacts of collapsing gullies on the dynamics of soil organic carbon in the red soil hilly region of southeast China. Catena 190. https://doi.org/10.1016/j.catena.2020.104547.

Zheng, L., Zhao, Q., Lin, G., Hong, X., Zeng, D. 2023. Nitrogen addition impacts on soil phosphorus transformations depending upon its influences on soil organic carbon and microbial biomass in temperate larch forests across northern China. Catena 230. https://doi.org/10.1016/j.catena.2023.107252.

1160 Zhou, T., Wang, C., Zhou, Z. 2020. Impacts of forest thinning on soil microbial community
1161 structure and extracellular enzyme activities: A global meta-analysis. Soil Biology and
1162 Biochemistry 149. https://doi.org/10.1016/j.soilbio.2020.107915.